NAVAL POSTGRADUATE SCHOOL

MONTEREY, CALIFORNIA

THESIS

DEVELOPMENT OF A SPHERICAL COMBUSTION CHAMBER FOR MEASURING LAMINAR FLAME SPEEDS IN NAVY BULK FUELS AND BIOFUEL BLENDS

by

Omari D. Buckley

December 2011

Thesis Co-Advisors: Knox T. Millsaps
Christopher M. Brophy

Approved for public release; distribution is unlimited

THIS PAGE INTENTIONALLY LEFT BLANK

REPORT DOCUMENTATION PAGE			Form Approved OMB No. 0704-0188
Public reporting burden for this collection of information is estimated to average 1 hour per response, including the time for reviewing instruction, searching existing data sources, gathering and maintaining the data needed, and completing and reviewing the collection of information. Send comments regarding this burden estimate or any other aspect of this collection of information, including suggestions for reducing this burden, to Washington headquarters Services, Directorate for Information Operations and Reports, 1215 Jefferson Davis Highway, Suite 1204, Arlington, VA22202-4302, and to the Office of Management and Budget, Paperwork Reduction Project (0704-0188) WashingtonDC20503.			
1. AGENCY USE ONLY ***(Leave blank)***	**2. REPORT DATE** December 2011	**3. REPORT TYPE AND DATES COVERED** Master's Thesis	
4. TITLE AND SUBTITLE Development of a Spherical Combustion Chamber for Measuring Laminar Flame Speeds in Navy Bulk Fuels and Biofuel Blends		**5. FUNDING NUMBERS**	
6. AUTHOR(S) Omari D. Buckley			
7. PERFORMING ORGANIZATION NAME(S) AND ADDRESS(ES) Naval Postgraduate School Monterey, CA93943-5000		**8. PERFORMING ORGANIZATION REPORT NUMBER**	
9. SPONSORING /MONITORING AGENCY NAME(S) AND DRESS(ES) Naval PostgraduateSchool Monterey, CA 93943-5000		**10. SPONSORING/MONITORING AGENCY REPORT NUMBER**	
11. SUPPLEMENTARY NOTES The views expressed in this thesis are those of the author and do not reflect the official policy or position of the Department of Defense or the U.S. Government.IRB Protocol number. IRB Protocol Number N/A_.			
12a. DISTRIBUTION / AVAILABILITY STATEMENT Approved for public release; distribution is unlimited		**12b. DISTRIBUTION CODE**	

13. ABSTRACT (maximum 200words)

This thesis presents the results of an experimental study to determine laminar flame speeds using the spherical flame method. An experimental combustion chamber, based on the constant-volume bomb method, was designed, built, and instrumented to conduct these experiments. Premixed Ethylene/air mixtures at a pressure of 2 atm, temperature of 298± 5K and equivalence ratios ranging from 0.8 to 1.5 were ignited and using a high speed video Schlieren system images were taken to measure the laminar flame speed in the expanding spherical flame front. The results were compared against published data for ethylene/air mixtures which yielded agreement within 5%.

An attempt was made to measure the laminar flame speed for F-76 at a pressure of 5 atm and temperature of 500K; however, premixed conditions were unable to be met due to auto-ignition and vapor characteristics of F-76. Suggestions for future work provide a potential solution and improvement to the current design.

4. SUBJECT TERMS Laminar Flame Speed, Spherical Flame Method, F-76, JP-5, Bio-Derived Fuels			**15. NUMBER OF PAGES** 83
			16. PRICE CODE
17. SECURITY CLASSIFICATION OF REPORT Unclassified	**18. SECURITY CLASSIFICATION OF THIS PAGE** Unclassified	**19. SECURITY CLASSIFICATION OF ABSTRACT** Unclassified	**20. LIMITATION OF ABSTRACT** UU

NSN 7540-01-280-5500 Standard Form 298 (Rev. 2-89)
Prescribed by ANSI Std. 239-18

THIS PAGE INTENTIONALLY LEFT BLANK

Approved for public release; distribution is unlimited

DEVELOPMENT OF A SPHERICAL COMBUSTION CHAMBER FOR MEASURING LAMINAR FLAME SPEEDS IN NAVY BULK FUELS AND BIOFUEL BLENDS

Omari Buckley
Lieutenant, United States Navy
B.S., Old Dominion University, 2004

Submitted in partial fulfillment of the
requirements for the degree of

MASTER OF SCIENCE IN MECHANICAL ENGINEERING

from the

NAVAL POSTGRADUATE SCHOOL
December 2011

Author: Omari D. Buckley

Approved by: Knox T. Millsaps
Thesis Co-Advisor

Christopher M. Brophy
Thesis Co-Advisor

Knox T. Millsaps
Chair, Department of Mechanical and Aerospace Engineering

THIS PAGE INTENTIONALLY LEFT BLANK

ABSTRACT

This thesis presents the results of an experimental study to determine laminar flame speeds using the spherical flame method. An experimental combustion chamber, based on the constant-volume bomb method, was designed, built, and instrumented to conduct these experiments. Premixed Ethylene/air mixtures at a pressure of 2 atm, temperature of 298± 5K and equivalence ratios ranging from 0.8 to 1.5 were ignited and high speed video was taken to measure the laminar flame speed in the expanding spherical flame front. The results were compared published known data for ethylene/air mixtures which yielded agreement within 5%.

An attempt was made to measure the laminar flame speed for F-76 at a pressure of 5 atm and temperature of 500K; however, premixed conditions were unable to be met due to auto-ignition and vapor characteristics of F-76. Suggestions for future work provide a potential solution and improvement to the current design.

THIS PAGE INTENTIONALLY LEFT BLANK

TABLE OF CONTENTS

THIS PAGE INTENTIONALLY LEFT BLANK

LIST OF FIGURES

LIST OF TABLES

THIS PAGE INTENTIONALLY LEFT BLANK

LIST OF ACRONYMS AND ABBREVIATIONS

bpd	Barrels per Day
Cequel	Chemical Equilibrium
DAQ	Data Acquisition
DoD	Department of Defense
Fps	Frames per Second
FT	Fisher-Tropsch
GUI	Graphic User Interface
HRD	Hydroprocessed Renewable Diesel
HRJ	Hydroprocessed Renewable Jet
LOWESS	Locally Weighted Scatterplot Smoothing
NPT	National Pipe Thread
SECNAV	Secretary of the Navy
SS	Stainless Steel
SSR	Solid State Relay
UNF	Unified Thread (Fine)
atm	Atmospheres
dr_f/dt	Flame front history (mm/s)
D_u	Mass diffusivity (mm^2/s)
in	Inches
K	Flame stretch rate (s^{-1})
KPa	KiloPascals
L	Markstein length (mm)
$Ma= L/\delta_D$	Markstein number (dimensionless)

mm	Millimeter
ms	Millisecond
psi	pound per square inch
r_f	Instantaneous flame radius (mm)
S_L	Stretched flame speed (mm/s)
S_u	Unstretched flame speed (mm/s)
δ_D	Characteristic flame thickness (mm)
ρ	Density
Φ	Fuel Equivalence ratio
	Subscripts
u	Unburned gas
b	Burned gas

ACKNOWLEDGMENTS

I would like to thank my thesis advisors Dr. Christopher Brophy and Dr. Knox Millsaps for giving me the opportunity to do research on such an exciting research topic. Their guidance and support provided an invaluable learning experience.

I would also like to thank Mr. Dave Dausen for sharing your electrical and technical knowledge associated with this research.

Thanks to Mr. George Hageman and Bobby Wright for always lending a hand in any work that I needed assistance with. The test would not have been a success without your help.

I would also like to thank Mrs. Emily Roncase for all her hard work. Her assistance was invaluable from the start of the program and I am positive she will be as instrumental as the research continues.

Special thanks to Dr. Jose Sinibaldi for his support and encouragement throughout the course of this thesis research

Finally, I would like to express my deep appreciation to my wife Stephanie and daughter Ramiyah for their support and understanding during this challenging time.

THIS PAGE INTENTIONALLY LEFT BLANK

I. INTRODUCTION

A. MOTIVATION

Petroleum-based fuel is a major driving force of our everyday life. It provides a major source of energy to manufacture and transport goods throughout the world.

However, in recent years growing environmental concerns, national security implications due to a finite supply, cost, and the need for a divers energy supply has led to the renewed interest in alternative fuels by the U.S. Department of Defense (DoD).

The United States Military depends on liquid hydrocarbon fuels for power and propulsion of many of its platforms and weapon systems, including surface ships, aircraft and cruise missiles. According to the National Defense Research Institute [1] the U.S. Navy consumes about 100,000 (bpd) barrels per day of jet fuel, JP-5 and JP-8, and 46,000 bpd of F-76 (DFM).

In response to the nation's growing environmental, economic, and security concerns on October 14, 2009, at the Naval Energy Forum, Secretary of the Navy (SECNAV) Ray Mabus announced the Navy's commitment to alternative and renewable energy [2]. The plan outlined stated that by 2015 the goal was to reduce petroleum fuel consumption by 50%, from 100,000 bpd to 50,000 bpd. By 2020, the aim is to have 40% of the Navy's total energy will come from alternative fuels and 50% of shore installations will come from renewable sources. He also commissioned a Green Strike Group, action ready by 2012, consisting of ships powered by nuclear and biofuel.

The Navy has made progress in its commitment to alternative fuels over past few years. On April 22, 2010 the successful test flight of the "Green Hornet" was conducted, it flew on a 50-50 blend of JP-5 and camelina derived Hydroprocessed Renewable Jet fuel (HRJ). Also on October 25, 2010, they conducted a successful test of a vessel powered by a 50-50 blend F-76 and algae-based renewable Diesel.

While biofuels have been tested in a number of systems there remain many unanswered questions as to the impact of using pure or blended biofuels in Navy systems as drop-in replacements. Along with long term fuel stability and the material compatibility issues with fuel systems, use in marine environments, and the physical and combustion characteristics may differ due to the slightly different change in chemical composition. While initial test in recent test in both the U.S. Navy and Air Force have been largely successful in demonstrating 50-50 blends in both biofuels and Fisher-Tropsch (FT), these where mostly short term demonstrations under normal conditions.

In order to deal with problems that may certainly arise with these new fuels a better fundamental understanding of their physical, chemical and combustion kinetics are needed. It is well known that both the Octane number in homogenous charge, spark ignition engine applications and Cetane number in Diesel engine applications are substantially influenced by fuel composition [3]. A key component to resolving this problem is to understand how the resulting chemical kinetic properties of the fuels, both blended and pure, influence

combustion behavior. This is achieved through developing and validating kinetic models.

The laminar flame speed is an important parameter when determining kinetic information of a combustible mixture. Laminar burning velocities of combustible mixtures have received attention as being: (1) a basic physiochemical property of the premixed combustible gases, (2) important in studying flame stabilization, (3) directly determines the rate of energy release during combustion, (4) a fundamental parameter that influence the performance and emissions of the combustion process in many combustion devices, (5) a property that affects the quench layer thickness, ignition delay time and ignition energy of the combustible mixture, and (6) needed to calibrate and validate the chemical reaction mechanisms for combustion simulations of different applications [4]. These models, based on the detailed kinetics information that the laminar flame speed provides, allow designers to better be able to optimize future engine designs. This need motivated the design for a spherical combustion chamber to measure the flame speeds of F-76, JP-5, Hydroprocessed renewable jet (HRJ) and Hydroprocessed renewable diesel (HRD) fuels to assist the U.S. Navy in gaining a better fundamental understanding of combustion characteristics of alternate fuels to be able to better screen future candidate fuels and identify potential problems such as flashback, blowoff, turbulent flame propagation, and in the “boundary” areas (low temperature and high altitude) where renewable fuels may have problems in critical operational environments.

B. LITERATURE REVIEW

Combustion is a very complex set of physical processes where long chain carbons react with mostly oxygen in the air in a progressive set of breaking chemical H-C bonds and recombining with available oxygen to form water and carbon dioxide. This literature review will look at some of the research that has been done relating to hydrocarbon/air flames, conventional and alternative jet fuels, previous findings and what remains to be unstudied.

The determination of laminar burning velocities can be determined using various approaches. There are five basic types of experiments to measure flame speeds as discussed by Kuo et al. [5], each utilizing different flame configurations, such as the spherical flame method, Bunsen-burner method, counterflow method, the flat-flame burner method and the transparent-tube method. Depending on the pressure, the spherical flame method can be conducted by either the constant-pressure or constant-volume method. The spherical flame method is not affected by the lack of uniformity of the laminar flame speed over the flame surface and can be performed at much higher pressures than the other methods allowing it to be a more desirable method for the current research.

Hassan et al. [6] studied the laminar burning velocities for premixed hydrocarbon/air flames at various pressures. Their research used the spherical flame method to find the sensitivities of laminar burning velocities to flame stretch as well as the fundamental laminar burning velocities of unstretched flames. They measured flame velocities for propane, ethylene, and ethane/air flames at

fuel-equivalence ratios of 0.8– 1.6, pressures of 0.5– 4.0 atm and temperatures at 298 ± 2 K. Their predictions were limited to unstretched flames using mechanisms based on GRI-Mech.

Figures 1-3 show their findings and those of Aung, [7] Taylor [8] and Egolfopoulos et al. [9] for the laminar burning velocities of propane, ethylene and ethane respectively. The data showed good comparison between measurements and predictions for the propane and ethane/air flames; however, the comparison between measurements and predictions is not as good for ethylene/air flames with predictions generally 20–30% greater than the measurements at fuel-rich conditions.

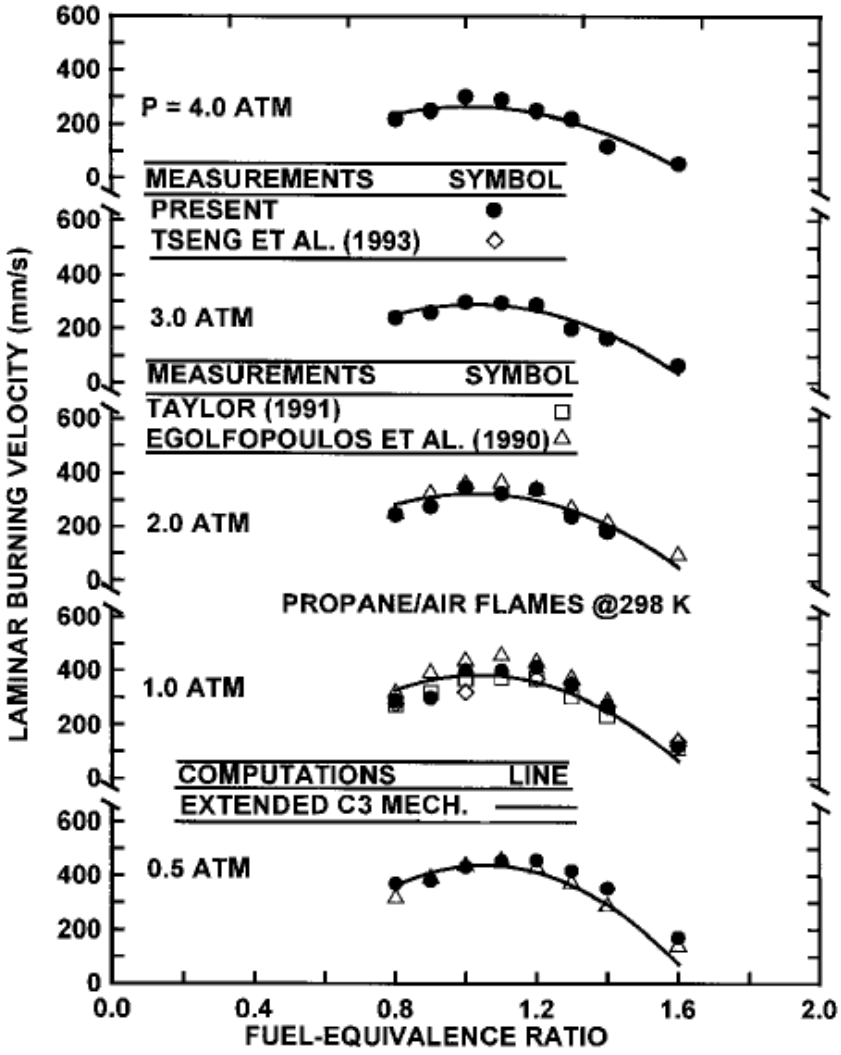

Figure 1. Measured and predicted laminar burning velocities as a function of fuel-equivalence ratio for propane/air flames at various pressures reproduced from [6]

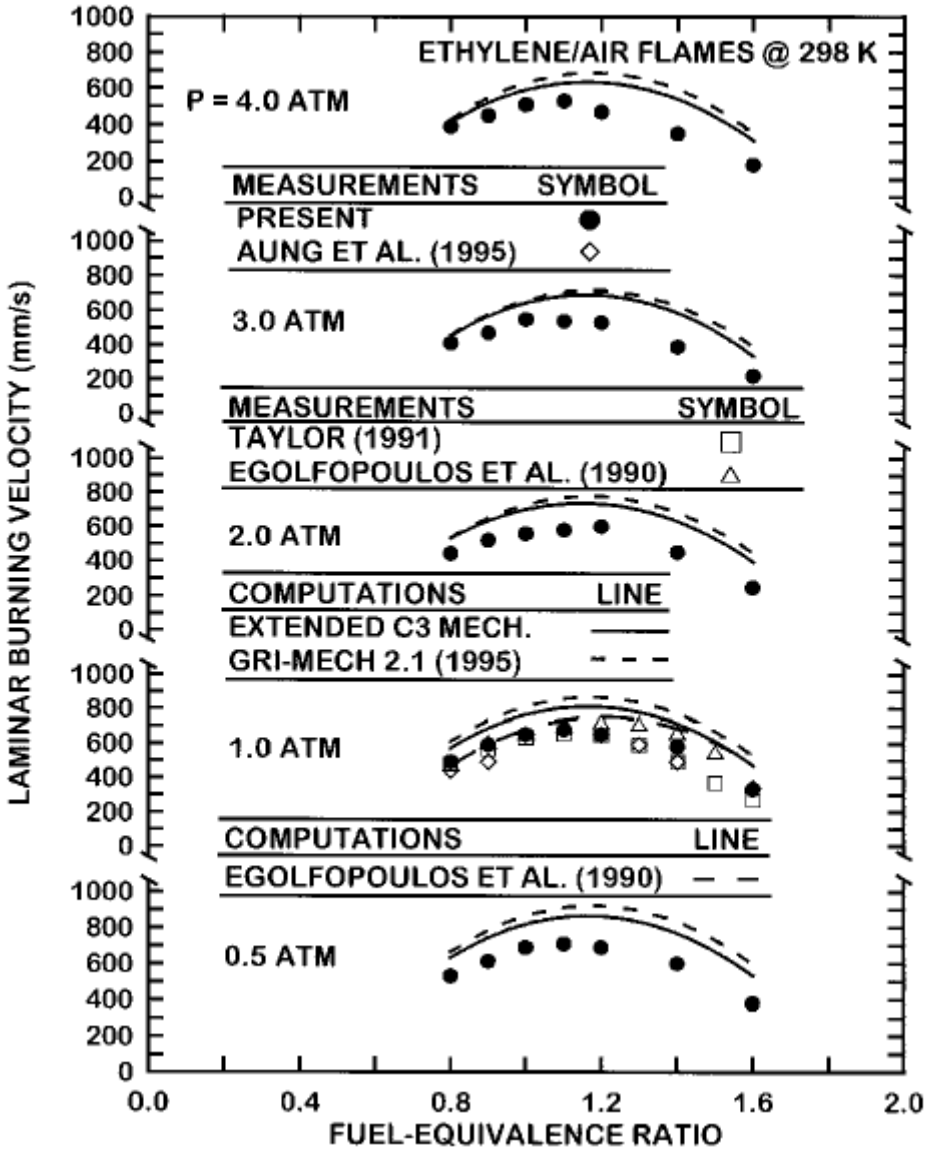

Figure 2. Measured and predicted laminar burning velocities as a function of fuel-equivalence ratio for ethylene/air flames at various pressures reproduced from [6]

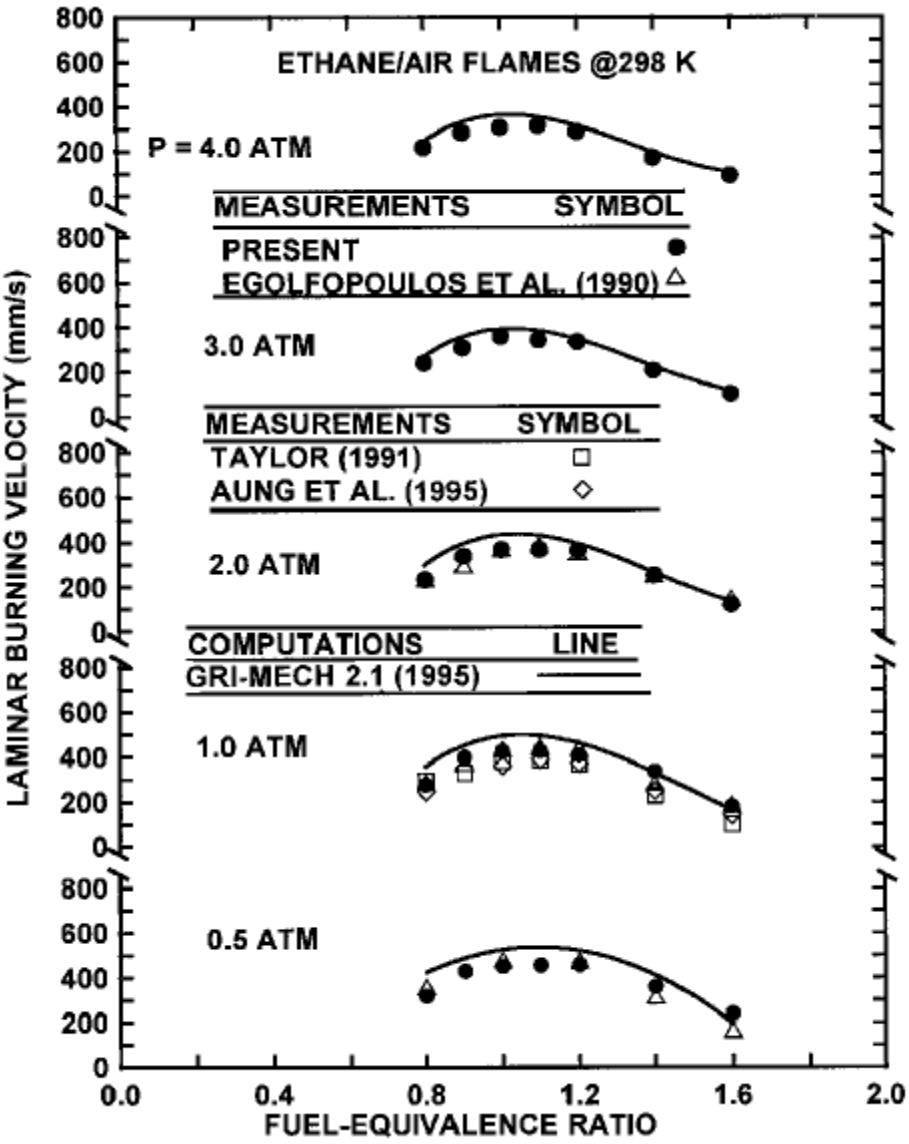

Figure 3. Measured and predicted laminar burning velocities as a function of fuel-equivalence ratio for ethane/air flames at various pressures reproduced from [6]

Hassan et al. research concluded that laminar burning velocities in the range of 220–450 mm/s for propane/air and ethylene/air flames and 390–710 mm/s for ethylene/air flames, respectively. They also noted that at modest pressures flames showed either stable preferential-

diffusion behavior at lean conditions for propane/air flames or near-neutral behavior as noticed in ethane and ethylene/air flames.

Egolfopoulos et al. [10] examined the laminar flame speeds of nonpremixed JP-7, JP-8, S-8 (Fischer-Tropsch fuel derived from natural gas by Syntroleum), R-8 (bioderived fuel, produced by Tyson, from animal/vegetable oil and subsequently deoxygenated) and Shell-GTL (Fischer-Tropsch fuel from gas to liquid, by Shell). The laminar flame speeds were determined using the counterflow technique at atmospheric pressure and elevated unburned reactant temperatures. Their results, Figure 4, show that JP-7/air and JP-8/air flames represented by a black triangle and black circle respectively, have a lower propagation speeds when compared to alternative fuels. Compared with *n*-paraffins (n-$C_{10}H_{22}$/air and n-$C_{12}H_{26}$/air represented by a white diamond and white square, respectively), S-8/air (black diamond), Shell-GTL/air (white triangle), and R-8/air (black square) flames exhibit similar unstretched laminar flame speeds, while JP-7/air and JP-8/air flames propagate, on average, 5% and 8% slower, respectively. Their maximum unstretched laminar flame speeds were 62.7, 62.9, 62.8, 60.6, and 58.5 cm/s for S-8/air, Shell-GTL/air, R-8/air, JP-7/air, and JP-8/air flames, respectively. They state that the relative magnitude of the unstretched laminar flame speed of the various fuels is largely caused by differences in the oxidation kinetics of the different compounds present in jet fuels.

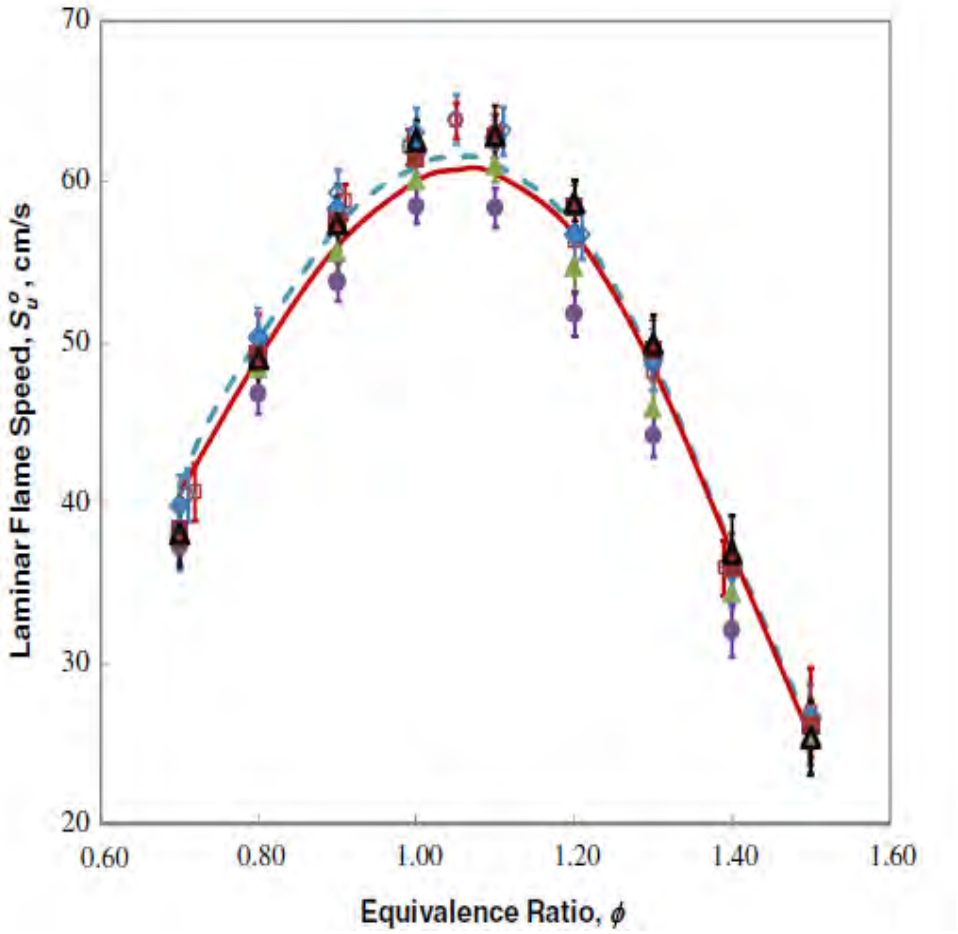

Figure 4. Experimentally determined laminar flame speed as a function of fuel-equivalence ratio JP-7/air, JP-8/air, S-8/air, Shell-GTL/air, R-8/air, n-$C_{10}H_{22}$/air, and n-$C_{12}H_{26}$/air and computed S°_{u} of n-C10H22=air and n-$C_{12}H_{26}$/air reproduced from [10].

The experimentation conducted by Egolfopoulos et al. [9], into the laminar flame speeds of JP-8 will provide a baseline for my current research into the expected laminar flame speed of JP-5 and HRJ. JP-5 and JP-8 have the same light carbon molecules and differ in the requirement of JP-5 to have a minimum flash point of 60°C (140°F). The addiction of an additive should only affect the flame speeds slightly and expected values should be close to that

of JP-8 at atmospheric pressure and elevated reactant temperatures.

Kuo et al. [5] notes that an increase in pressure is expected to increase the overall reaction rate and, hence, increase the laminar flame speed. He also notes that the preheat temperature influences the laminar flame speed mainly through the changes in reaction rate and diffusive properties. The rate of increase for the adiabatic temperature is more for lean mixtures than for stoichiometric or rich mixtures. Therefore, the expected laminar flames of JP-5 and F-76 should be higher than those measured by. Egolfopoulos et al. [9].

To the best of the author's knowledge there is no open source literature pertaining to the laminar flame speeds of F-76/Air, JP-5/air, HRJ/Air or HRD/Air mixtures conducted at high temperature and pressures.

C. OBJECTIVES

The objectives of this research are to:

1. Design, build, and calibrate a temperature controlled high pressure combustion chamber used for measuring laminar flame speeds of Navy Bulk Fuel and Bioblends.
2. Measure laminar flame speeds of Ethylene/Air mixtures at 2 atm, 298 ± 5K and equivalence ratios from 0.8-1.5 and compare with published data.
3. Measure laminar flame speeds of F-76/Air mixture at 5 atm, 500 K, and equivalence ratios from 0.8-1.5.

D. ORGANIZATION

Chapter II describes the design concept, components, and data acquisition process used for measuring laminar flame speeds.

Chapter III presents the method for calculating laminar flame speed using the spherical bomb method and the method of data reduction.

Chapter IV presents and discusses the results of the experiments.

Chapter V provides conclusions and recommendations for future work.

II. EXPERIMENTAL APPARATUS

The experimental combustion chamber is comprised of 7 main modules: a) combustion chamber, b) fuel vaporization and supply system, c) air supply system, c) spark ignition system, d) exhaust system, e) a high-speed Schlieren imaging system and f) a control system. The complete experimental setup is shown in Figure 5. The material specifications, analysis and components, as well as the design considerations, are described in this section.

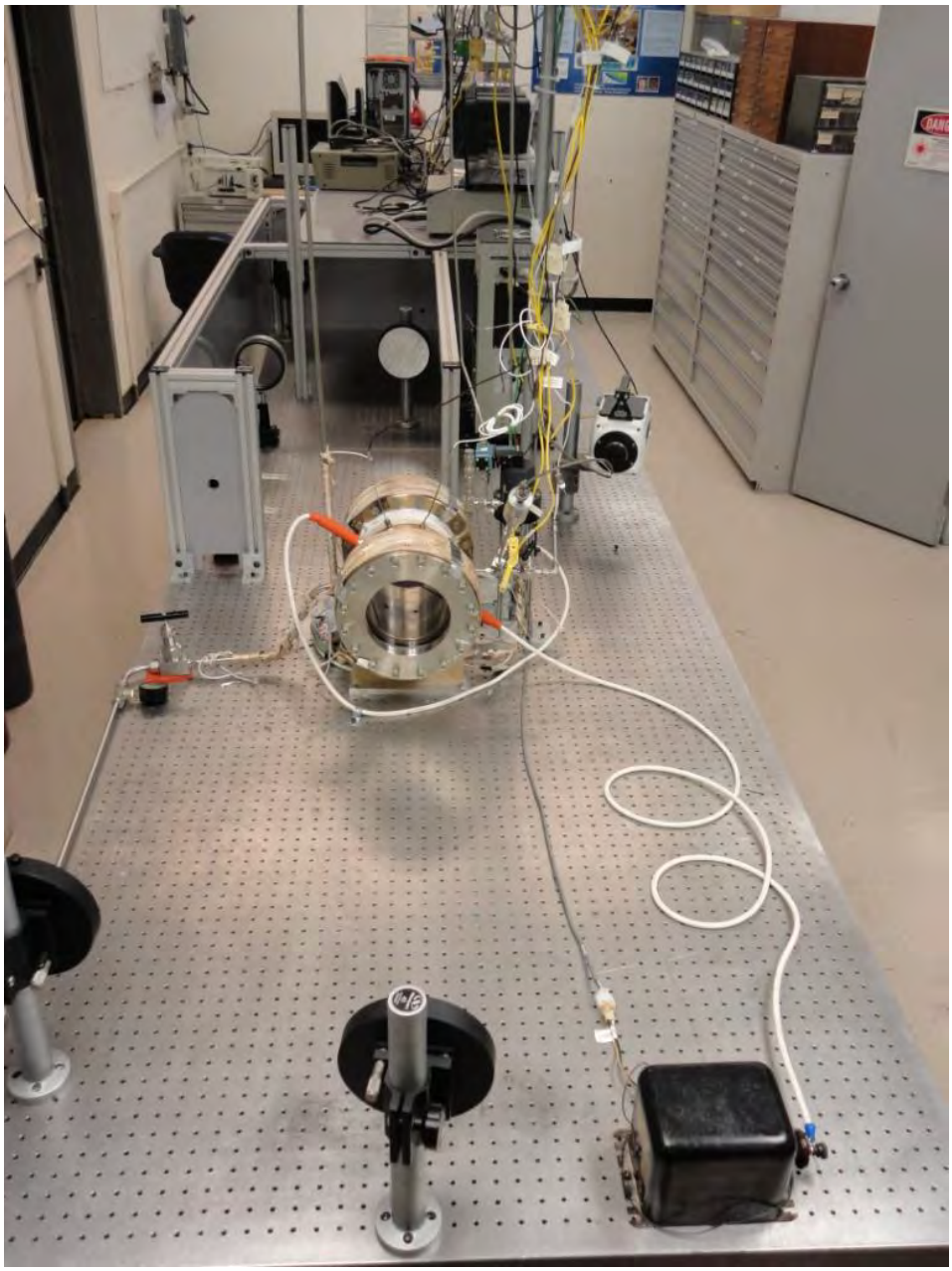

Figure 5. Layout of Experimental Set-up

A. COMBUSTION CHAMBER

The combustion chamber, shown in Figure 6, was designed for initial pressures less than 20 atm and initial

temperatures up to 500 K testing. The center chamber was machined out of a single piece of stainless steel (SS-304) to prevent any weakness introduced by potential imperfections in welds and miss alignments. It has dimensions of 125 mm and 209.5 mm (6in and 8.25in) for internal and external diameters respectively with a total length of 203.2 mm (8 in) in length including the flange ends. The chamber has a total volume of 3.2 liters (196.6 in^3). The material selection of Stainless steel was primarily based on its chemical inertness, structural rigidity and strength.

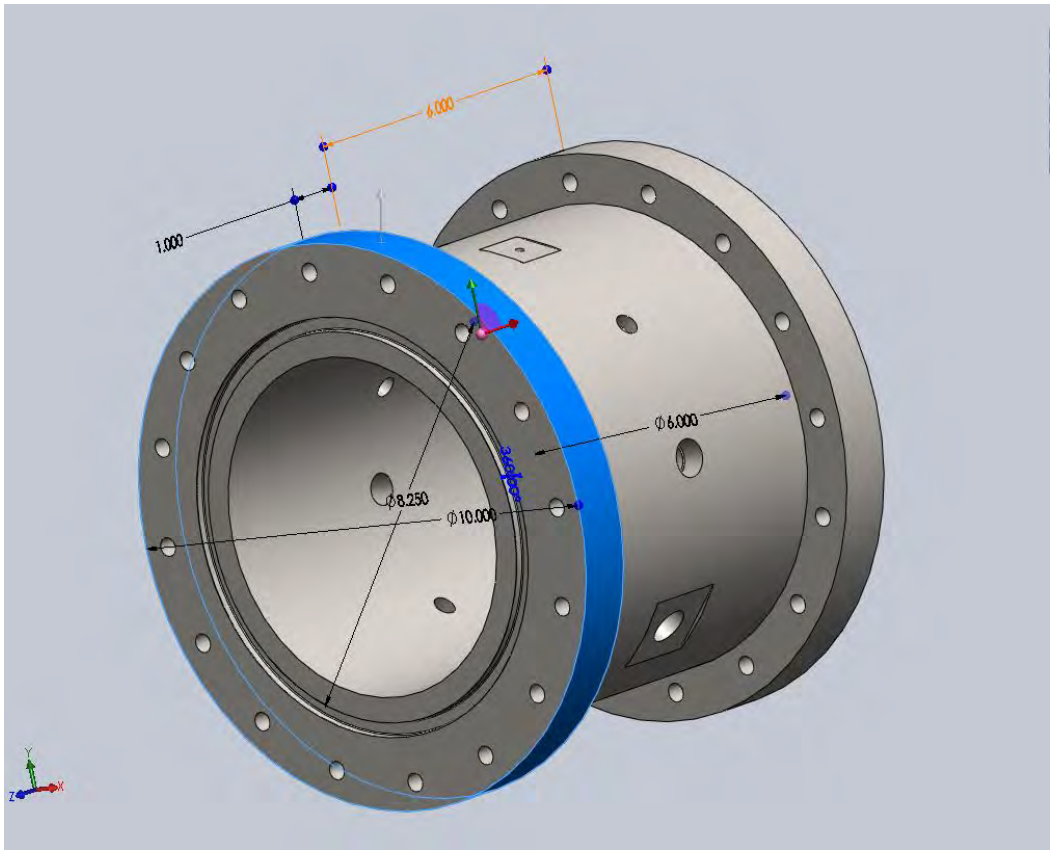

Figure 6. Center Combustion Chamber

The chamber has 9 ports (see Appendix) aligned along its central plane: 1) two high voltage electrode ports, 2)

two pressure transducer ports (partial pressure, and reaction measurement), 3) one fuel feed line port, 4) one air feed line, 5) one vacuum pump port, 6) one thermocouple port and 6) one exhaust port. These ports utilize national pipe thread (NPT) connectors, Swagelok fittings and stainless steel tubing to connect the auxiliary systems to the chamber.

1. Window and Flanges

Two 203.2 mm (8 in) diameter and 50.8 mm (2 in) thick A1 optical fused quartz windows (Figure 7) are mounted on opposite ends of the center chamber via window flanges (Figure 8). The windows have a high fidelity transmission of light in the visible spectrum and designed to withstand pressure up to 17.27 KPa (2500 psi). Due to the physical properties of fused Quartz it cannot have direct contact with the metal surfaces at high temperatures. To prevent failure a flat gasket was placed between the outer face of the flange, an O-ring between the window and the chamber end and silicon tape between the window side wall and the flange sidewall.

The window flanges were made from a 254 mm (10 in) outer diameter SS-304 bar stock (Figure 8). This secures the windows against the flanged ends of the chamber, compressing the O-ring between the window and the chamber end. The 152.4 mm (6in) viewport provides unrestricted visibility of the inside of the chamber.

Figure 7. Optical Window

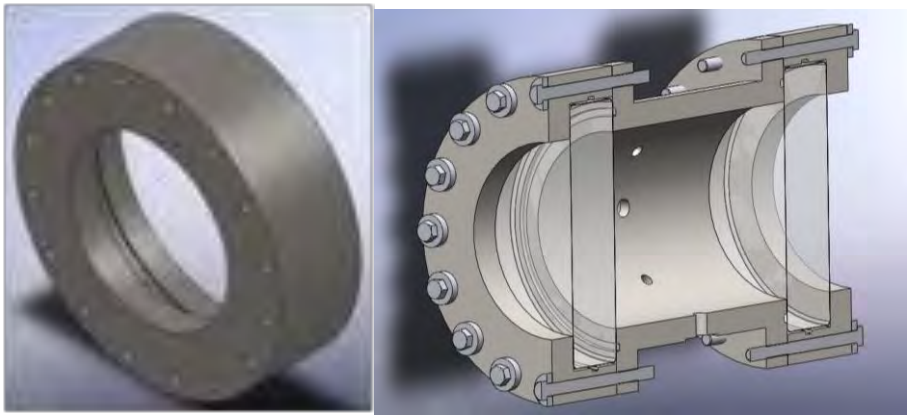

Figure 8. Optical Window Flange

2. Pressure Transducers

Two super high temperature low G sensitivity pressure transducers were flush mounted on the chamber. One pressure transducer (make: Kulite, model: XTEH-10L-190-500A, Pressure Range: 0 to 35 bar (0-500 psia), Temperature Range: 26°C-454°C(80°F-850°F), accuracy: ±0.1% FSO) was used for measuring both the chamber pressure during the gas fill process and the dynamic pressure history during combustion. The other transducer was used for measuring the partial pressures during the gas-filling process (make: Kulite, model: XTEL-190-15A, Pressure Range: 0 to 2 bar (0-

30 psia), Temperature Range: 26°C-454°C (80°F-850°F), accuracy: ±0.1% FSO). To isolate and prevent the partial pressure transducer from being damaged during experimental operations, due to maximum pressure range of transducer, a severe service needle valve (Swagelok SS-3NRS4-G) and pressure adapter (see appendix for dimensions) were used. Figure 9 depicts the instrumentations described above.

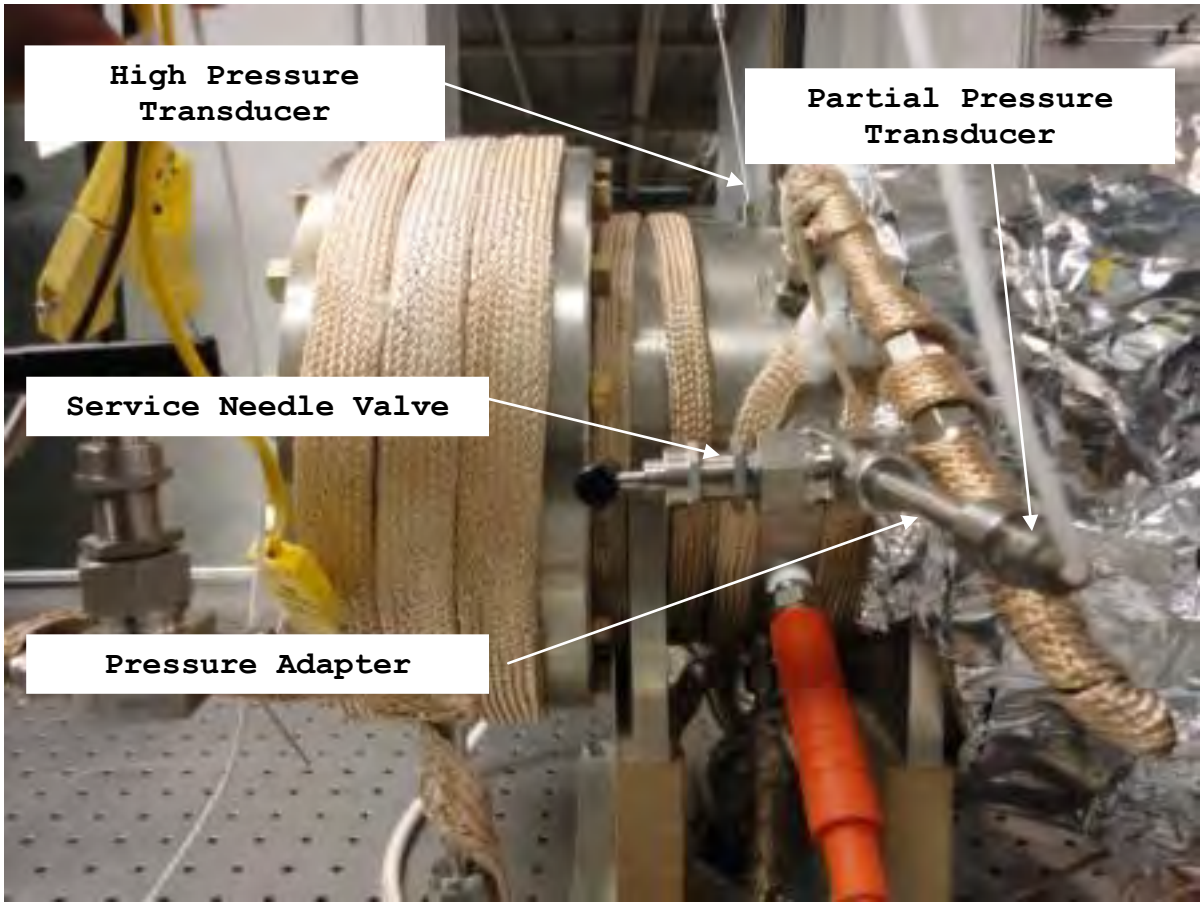

Figure 9. Pressure Measuring Instrumentation

3. Thermocouples

A 1.575 mm (0.062 in) Diameter 152.4 mm (6 in) Long Inconel Sheathed Type K Thermocouple (Figure 10) (make: TC

Measurement and Control Inc., Range: 0-1098.89°C (0-2010°F) was used to measure the initial temperature of the reactant mixture. A 1.575 mm x 3.175 mm (0.062 in x 0.125 in) NPT stainless steel compression fitting was used to secure the thermocouple to the chamber body.

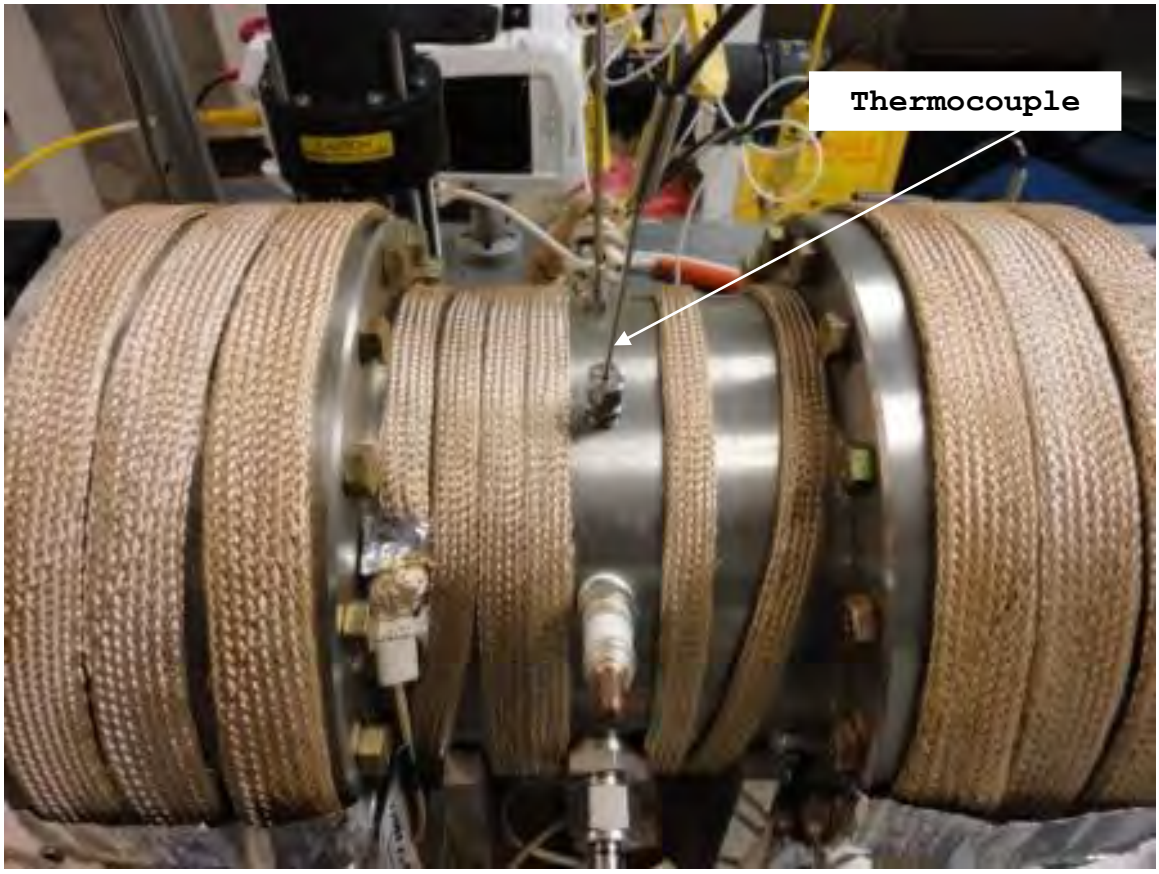

Figure 10. Thermocouple

B. SUPPLY SYSTEM

1. Fuel Vaporization and Supply System

The fuel vaporization and supply system (Figure 11) consist of a single fuel tank (Figures 12 and 13), machined from a single round stock of SS-304, with a lid (Figure 14)

connected to the combustion chamber by a Swagelok fitting (Swagelok SS-400-1-OR), 6.35 mm (0.25 in) 316 outer diameter stainless steel tubing, a severe service needle valve (Swagelok SS-3NRS4-G), heating tape (make: Omega, model:STH051-060), 12.70 mm (0.5 in) thermal blanket (make: Isofrax, model: 1260C, melting point: 1,499°C (2,730°F), K-type thermocouples and temperature controllers (make: Omega, model: CNI8DH44-EI). The fuel tank and the stainless steel tubing are wrapped with the heating tape with a thermocouple placed on the line from the fuel tank to the combustion chamber to ensure uniform temperature along the line. The fuel tank has a volume of 0.128 liters (7.854 in^3). The pressure of the vaporized fuel in the tank is measured by a pressure transducer (make: Kulite, model: XTEL-190-15A, Pressure Range: 0 to 2 bar (0-30 psia), Temperature Range: 26°C-232°C (80°F-450°F), accuracy: ±0.1% FSO) via a 4.039 mm (0.159 in) diameter hole with M5 x 0.08 UNF (10-32 UNF).

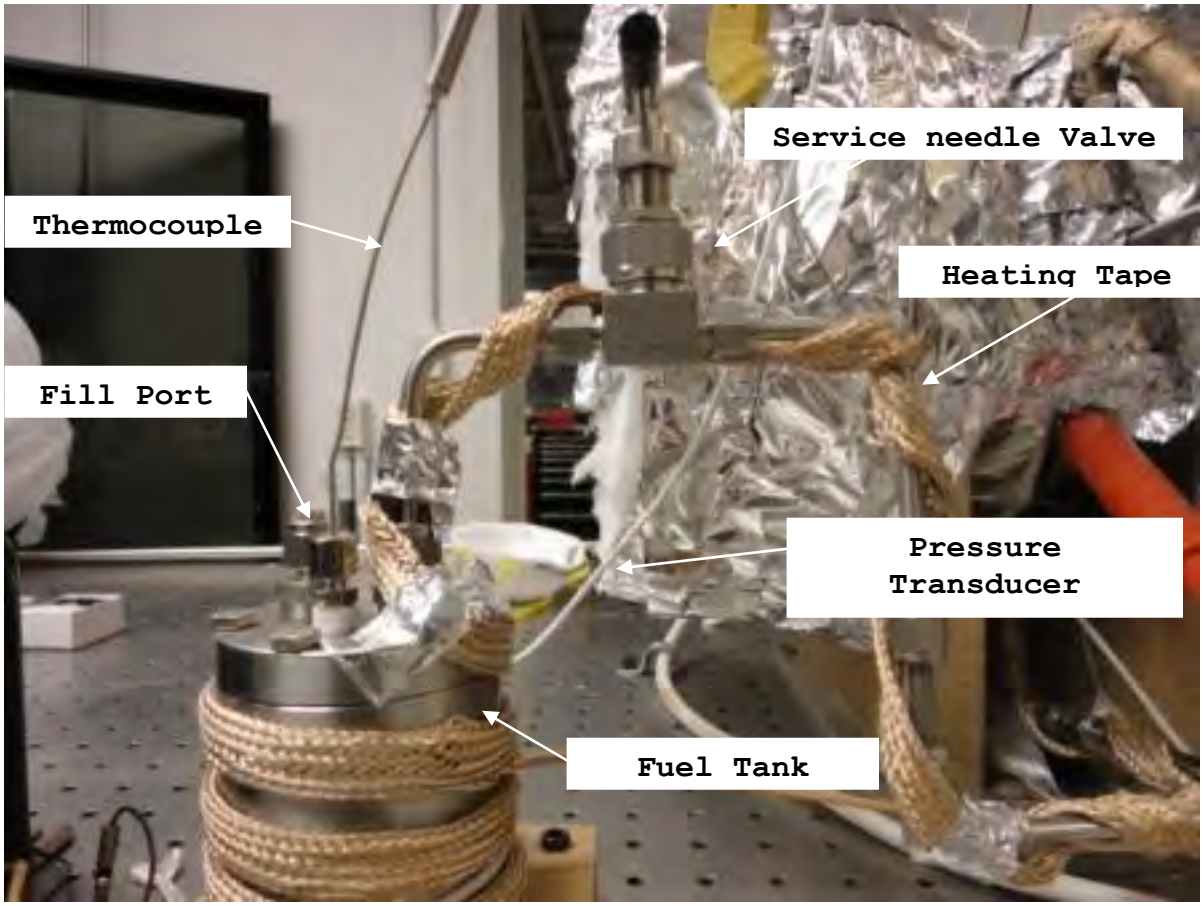

Figure 11. Fuel Vaporization and Supply System

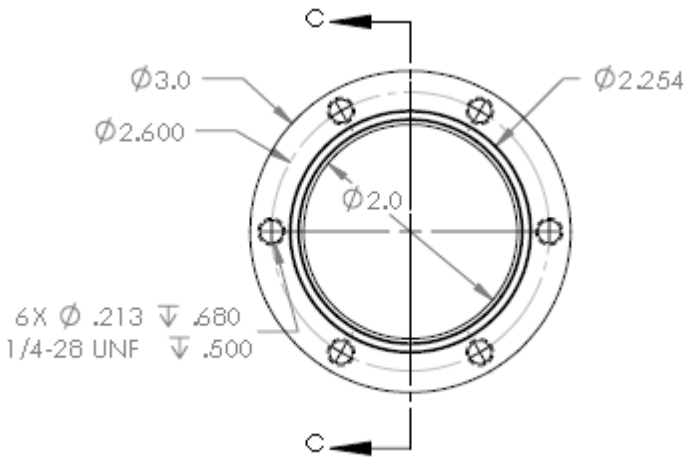

Figure 12. Fuel Tank Dimensions (All Dimensions In Inches)

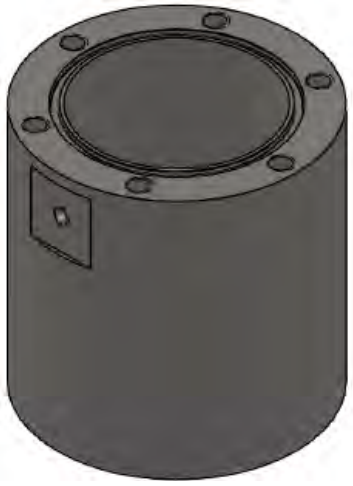

Figure 13. Fuel Tank

The fuel tank lid has 3 ports: 1) Fuel fill port, 2) Fuel exit port 3) and a Thermocouple port. The two 9.931 mm (0.391 in) diameter holes with M12 x 1.75 UNF (0.4375-20 UNF) were used for the fuel fill and exit ports. Both ports are connected flush to the fuel lid via 6.35 mm (0.25 in) straight Swagelok fitting (SS-400-1-OR). A 1.575 mm (0.062 in) Diameter 152.4 mm (6 in) Long Inconel Sheathed Type K

Thermocouple (make: TC Measurement and Control Inc., Range: 0-1098.89°C (0-2010°F) was used to measure the temperature of the fuel in the tank. A 1.575 mm x 3.175 mm (0.062 in x 0.125 in) NPT stainless steel compression fitting was used to secure the thermocouple to the fuel tank lid.

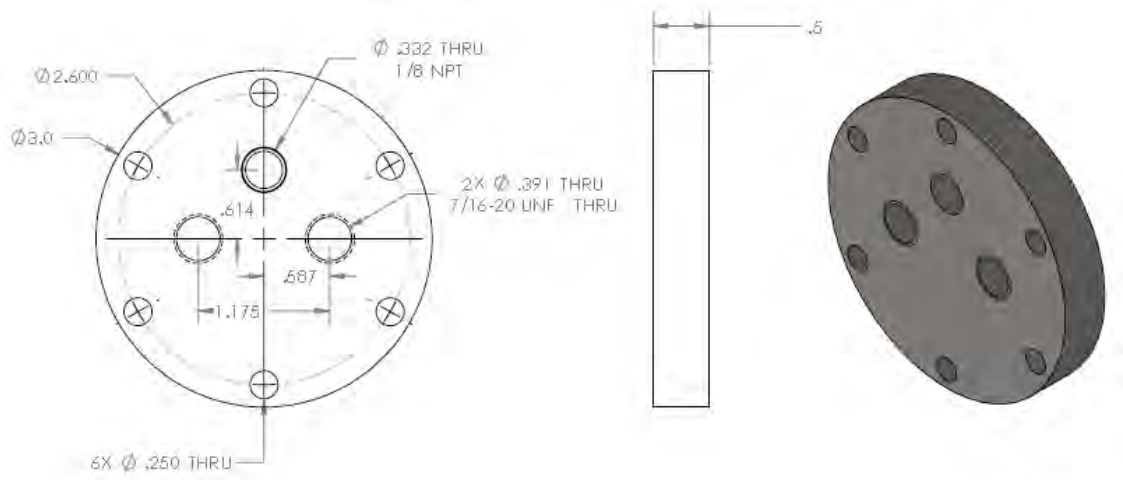

Figure 14. Fuel Tank Lid (All dimensions In Inches)

2. Air Supply System

The air supply system to the combustion chamber consists of a compressed air tank (Figure 15) with a regulator(Matheson-tri-gas 3040-CGA-580) to deliver air pressure from 689.47 to 17,236.89 KPa(100 to 2500 psig). Compressed air is delivered through 9.525 mm (0.375 in) stainless steel tubing to an electro-pneumatic ball valve (Swagelok SS-43GS6-33C) and a 24 VDC electronic controlled micro-solenoid (Figure 16) that is used to control the flow of air (oxidizer) into the combustion chamber. A check valve (Swagelok SS-56S6) upstream (Figure 17) of the flow prevents backflow. Heating tape (make: Omega, model: STH051-060) was placed around the 9.525 mm

(0.375 in) tubing, near the combustion chamber, to allow for uniform heating into the chamber.

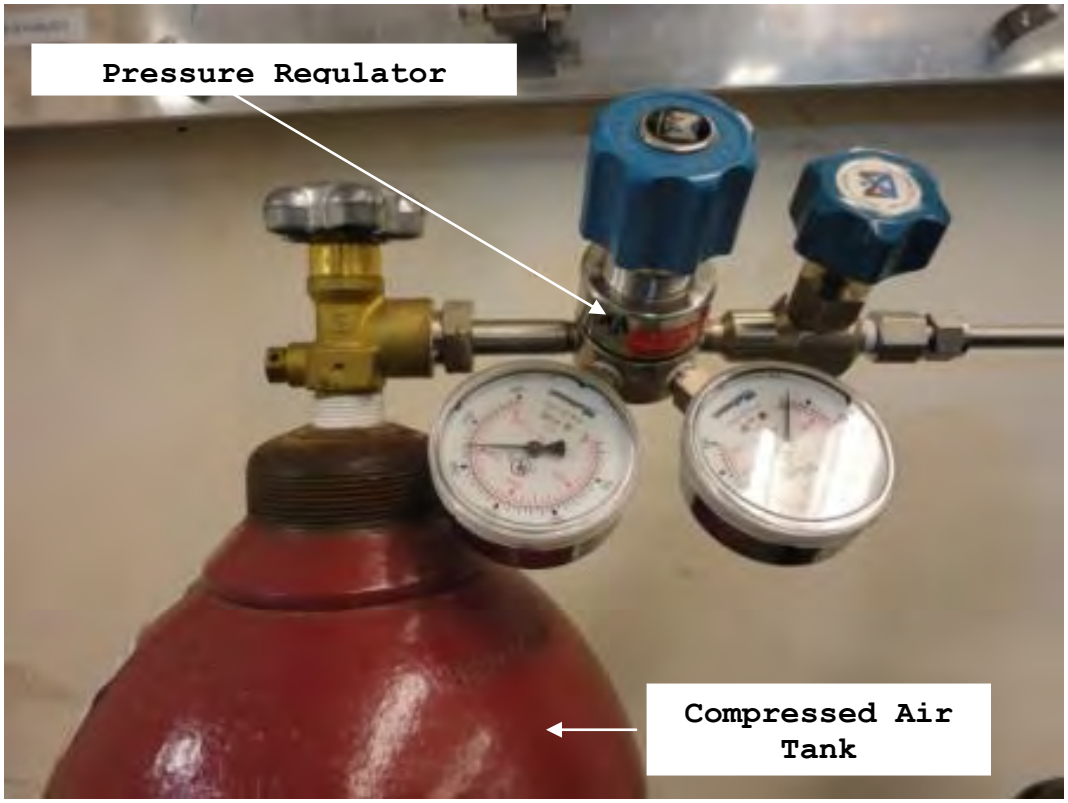

Figure 15. Compressed Air Tank and Pressure Regulator

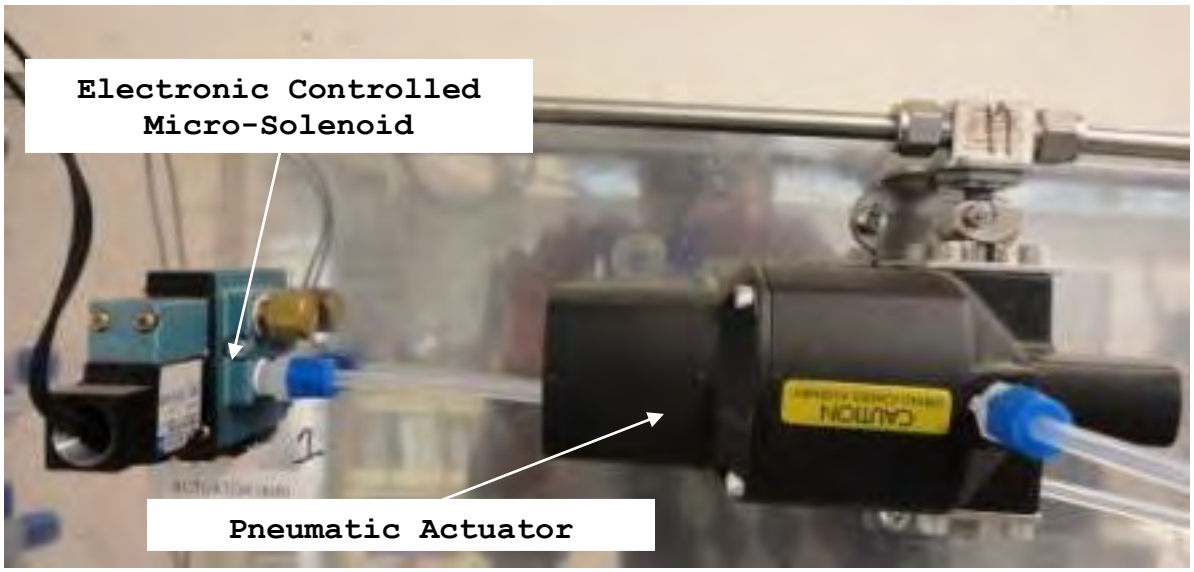

Figure 16. Swagelok Electro-pneumatic Ball Valves

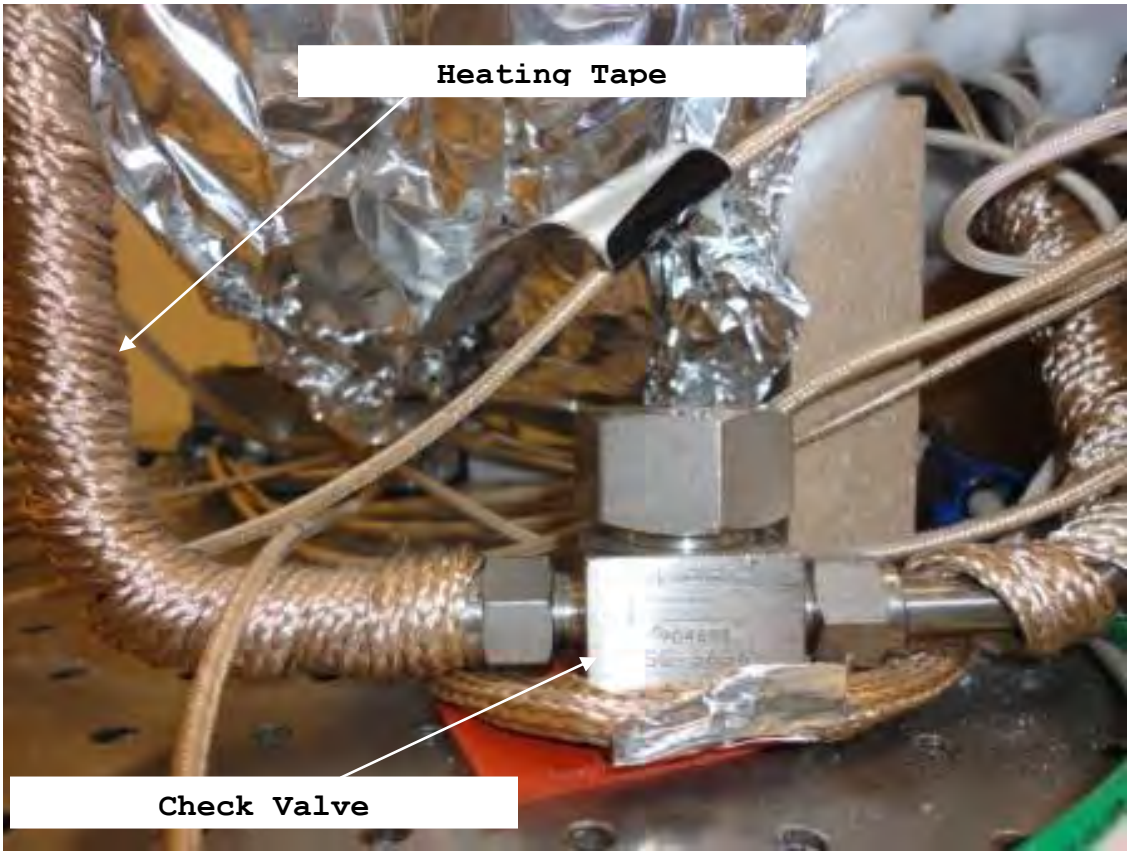

Figure 17. Air Feed Line Check Valve and Heating Tape

C. IGNITION SYSTEM

Central ignition of theunburned gas mixtures was carried out by electronic spark ignition through two extended electrodes (Figure 18), machined to specifications, (make: Ceramtec, model: 21143-01-A)with copper conductors fixed at diametrically opposite points on the pressure vessel via 9.525 mm (0.375 in) NPT ports. The electrodes were fixed and hence, the electrodes were machined to have a gap of 1 mm (0.03937 in).

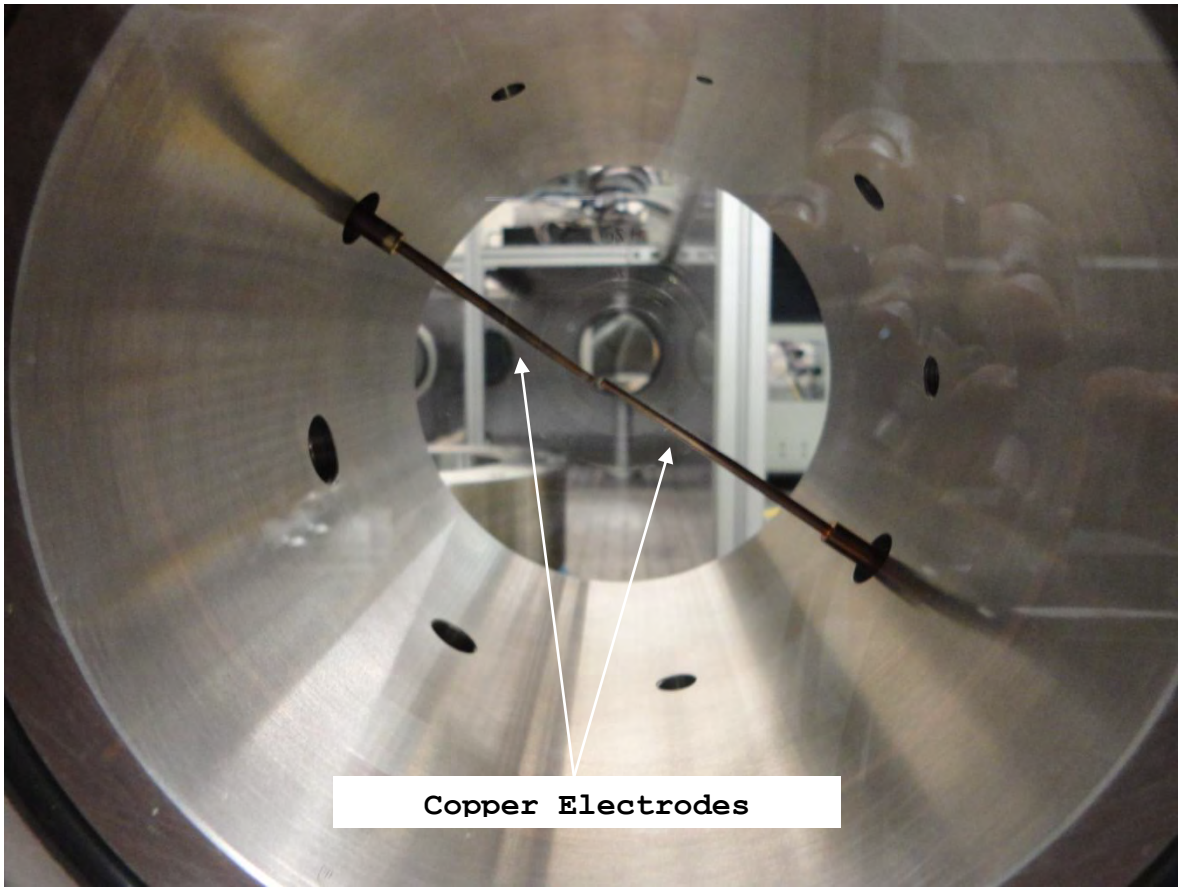

Figure 18. Copper Electrodes Mounted on the Combustion Chamber

A single spark ignition transformer (Figure 19) was used to generate the required voltage across the copper electrodes. When ignition is triggered in the control code a signal is sent to the solid state relay (make: Crydome, D1225) triggering 120 V to be sent to the transformer. The voltage is then relayed via the high voltage cables to the copper electrodes, creating a spark at the tip of the electrodes.

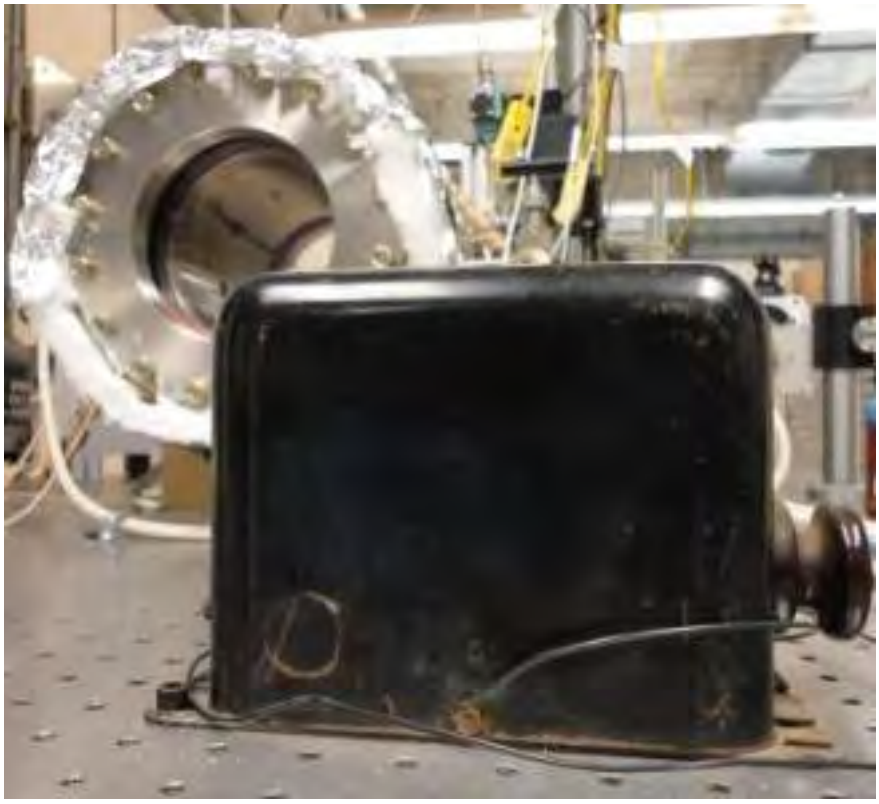

Figure 19. Ignition Transformer

D. SCHLIEREN SYSTEM

The general optical setup is a Z-type Schlieren configuration (Figure 20) equipped with a 1,600 Watt mercury/xenon arc lamp (Figure 21) (make: Newport Oriel Instruments, model 66870) in combination with a constant-current DC power supply (make: Newport Oriel Instruments, model 69922) (Figure 22).The light is initially steered off the first two flat mirrors through a condenser lens and a spatial filter to clean up the light by filter out excess light and focusing the light to a single point. The light is then reflected off another spherical mirror to a flat mirror through the combustion chamber to a spherical mirror. The flame propagation is then captured using a high-speed digital

camera (Figure 24) (make: Vision Research, model: Phantom v311) at 1,024 x 800 resolution at a frame rate set to 3,200 fps.

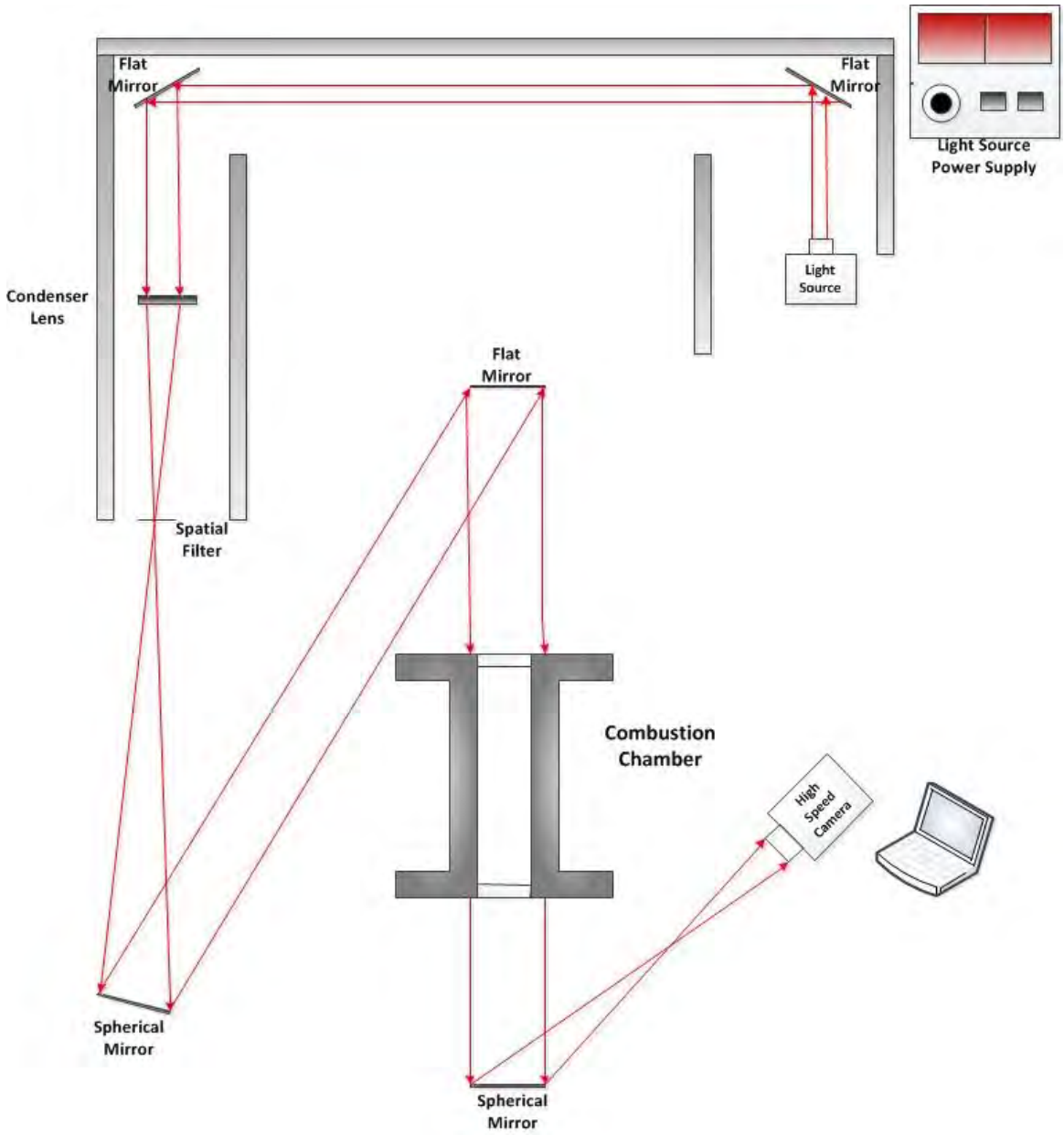

Figure 20. Z-Type Schlieren System Configuration

Figure 21. Mercury/xenon Arc Lamp

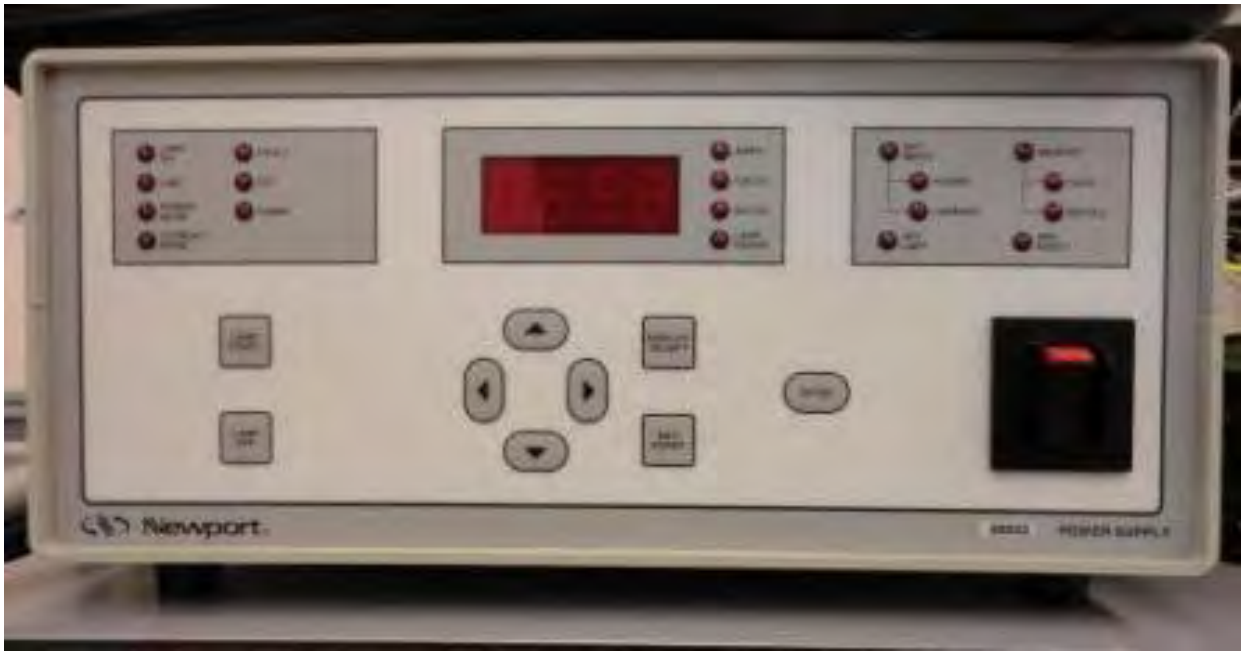

Figure 22. Arc Lamp Power Supply

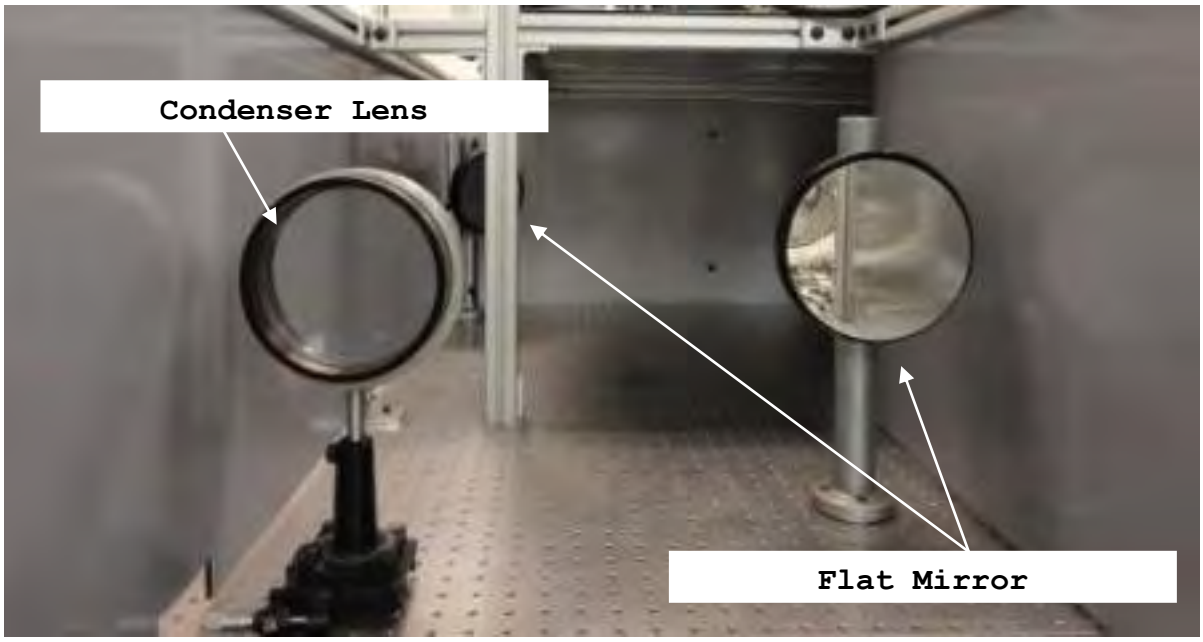

Figure 23. Spherical Mirror and Condenser Lens

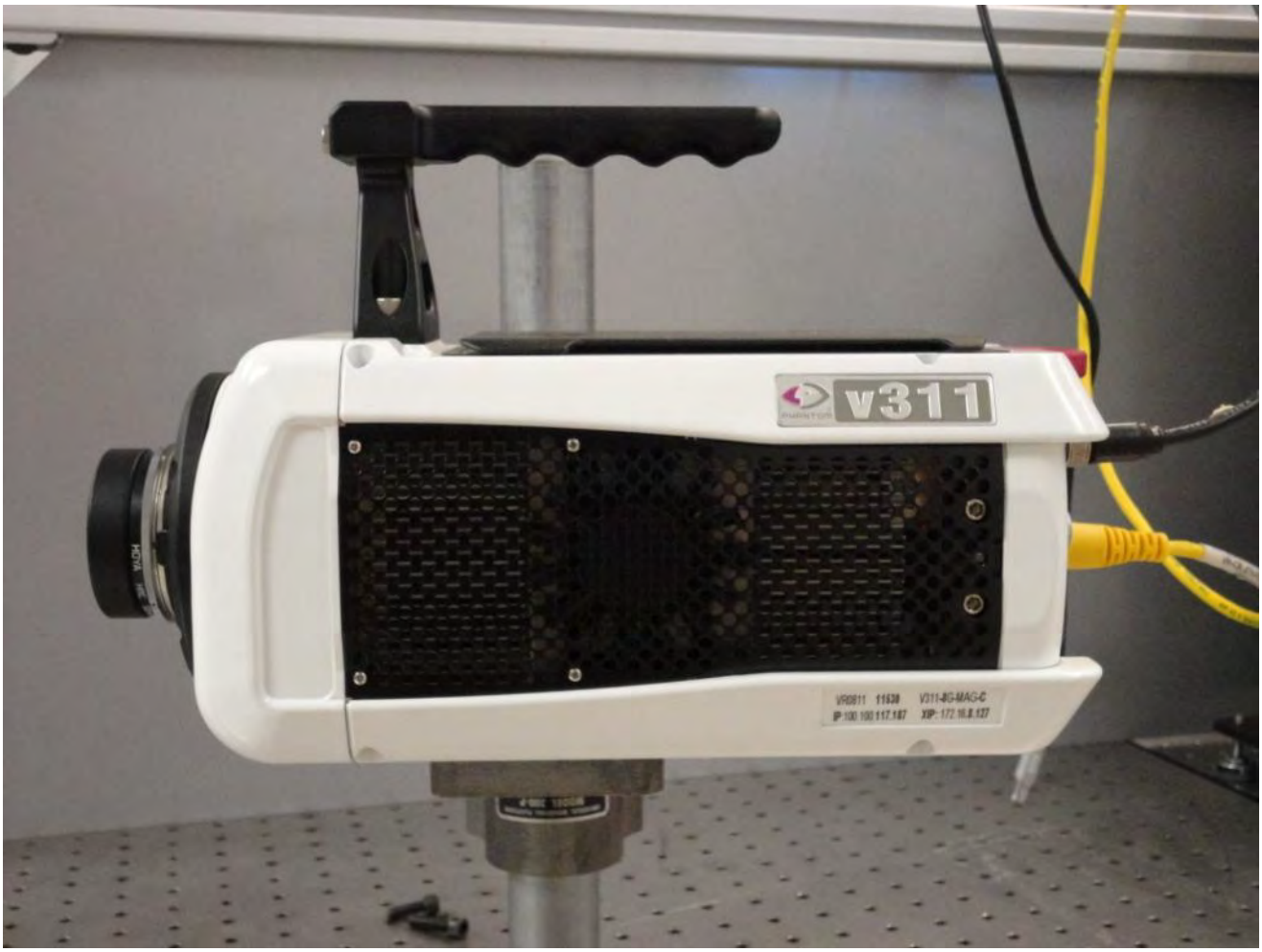

Figure 24. Phantom v311 High Speed Digital Camera

E. EXHAUST SYSTEM

The exhaust system (Figure 25) is connected to the combustion chamber via a M12 x 1.75 UNF (0.4375-20 UNF) through hole for a 6.35 mm (0.25 in) Swagelok fitting allowing for the products of combustion to be vented after each test. The system consists of 6.35 mm (0.25 in) stainless steel tubing, heating tape (make: Omega, model: STH051-060), a Severe-Service Union-Bonnet Needle Valve

(make: Swagelok, model: SS-3NRS4-G-95C-12453) and a 24VDC electronic controlled micro-solenoid.

Figure 25. Exhaust System

F. VACUUM SYSTEM

.The Vacuum system is connected to the combustion chamber via a M20 x 2.5 UNF (0.75-16 UNF) through hole for a 12.7 mm (0.50 in) Swagelok fitting and is used to evacuate the combustion chamber before the unburned gas filling process. The system consists of 12.7 mm 316 stainless steel tubing, severe service needle valve (make:

Swagelok, model: SS-6NRS8-G), a vacuum gauge (Figure 26) and vacuum pump.

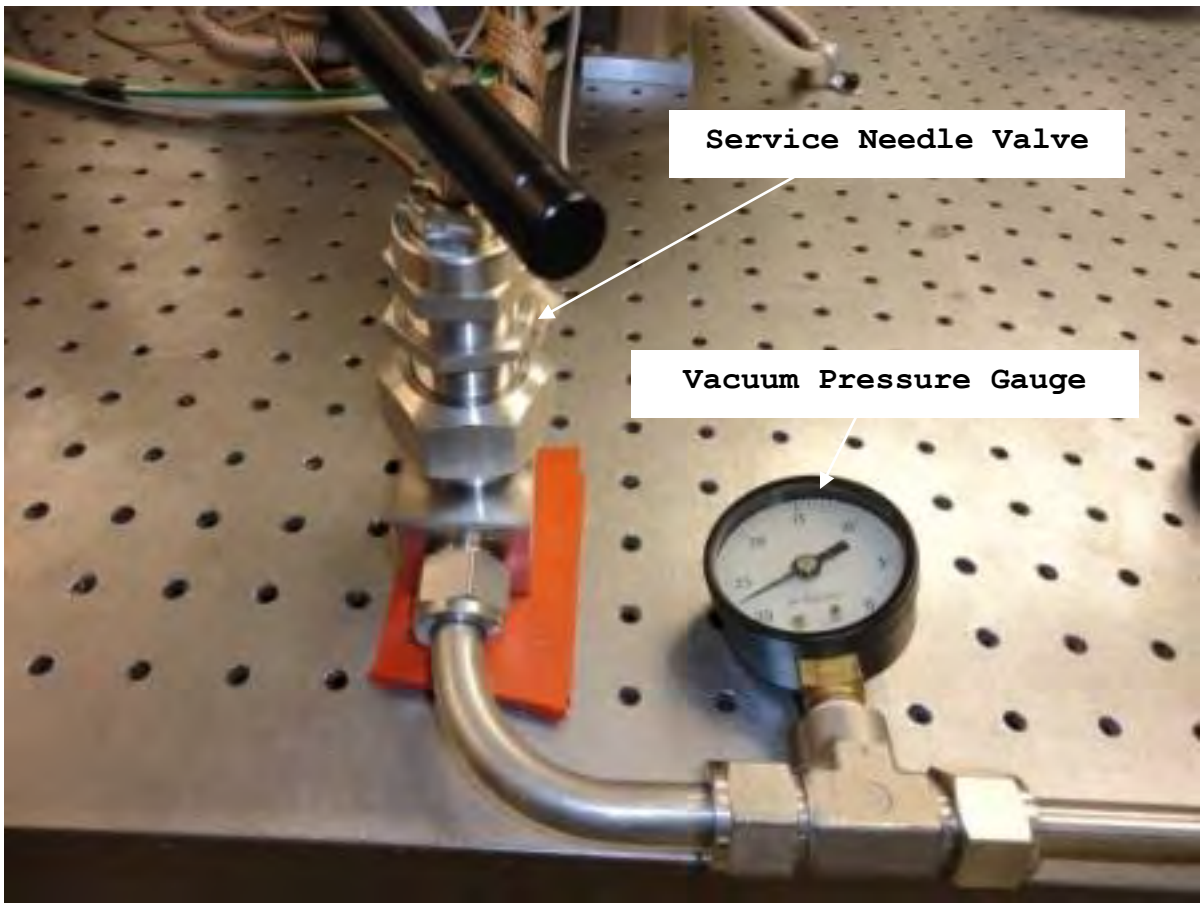

Figure 26. Vacuum System Service Needle Valve and Pressure Gauge

G. HEATING AND CONTROL SYSTEM

The heating and control system (Figure 27) is used to heat the combustion chamber as well as all of its auxiliary lines to a uniform temperature prior to combustion. It also records the pressure and temperatures throughout the fill and combustion processes. The system is comprised of heating tape (refer to previous subsystems), 4 Omega solid-state relays (SSR) (make: Omega, model: SSRL240DC100), 2 finned heat sinks (make: Omega, model: FHS-6), 4

temperature heat tape controllers (make: Omega, model: CNI8DH44-EI), 3 pressure displays (make: Omega, model: DP25B-S-A), 1 temperature display (make: Omega, model: CNI832), a 24 VDC power supply and a 5VDC power supply.

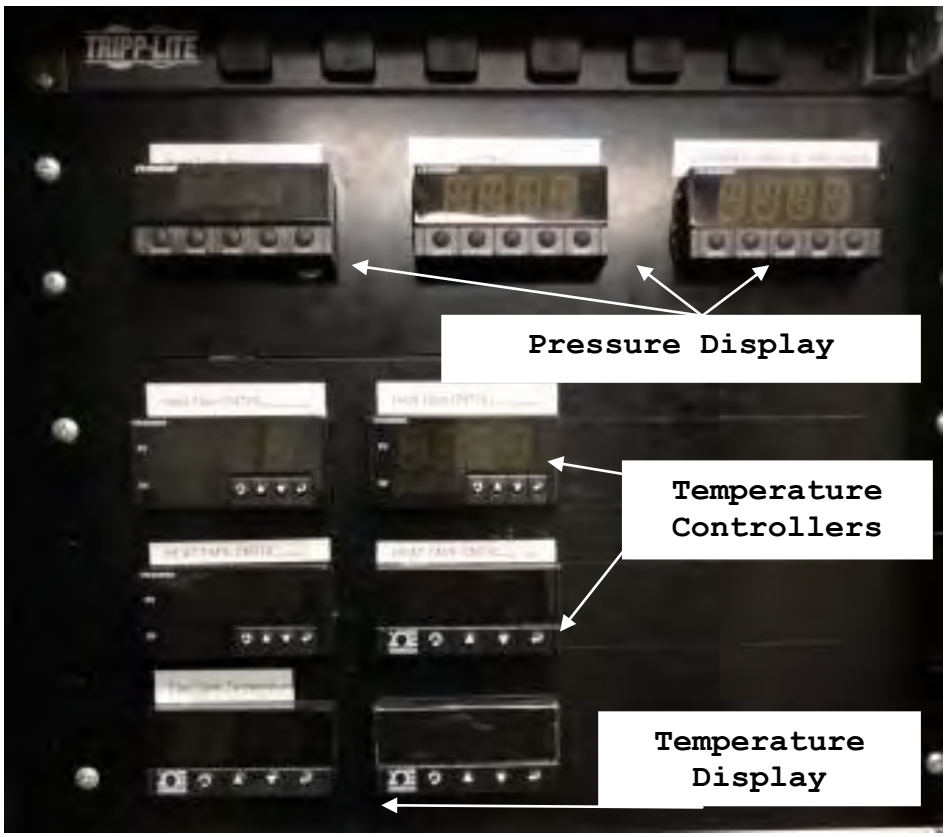

Figure 27. Heating and Control System

The heating tape for the center chamber and all of the auxiliary lines are connected to SSR (Figure 28) via one pin on the load side of the relay, the other is used to provide either 120V or 240V to the heating system. The control side connects to the Omega controllers. The temperature is regulated by preset temperatures programmed into the controllers and K-type thermocouples that act as a

feedback input to the controller, where a control signal causes the SSR to switch the load on or off.

Figure 28. Solid State Relays and Finned Heat Sinks

The pressures in the chamber and fuel tank are monitored with three omega pressure display units. The displayed pressures are then retransmitted across BNC cables to a data acquisition system (DAQ). This DAQ allows for the pressure to me monitored and recorded via a National Instrument Graphical User Interface (GUI) program (Figure 30).

Figure 29. National Instrument Data Acquisition System

The National Instruments LabView program and the control box depicted in Figure 27 serve as a centralized controller for the air and exhaust actuators. The air and exhaust solenoid valves are electrically wired and controlled by CRYDOM SSR's. A 24VDC power supply provides power to the solenoid valves and the 5V DC used to supply power to the SSR's are provided by the DAQ.

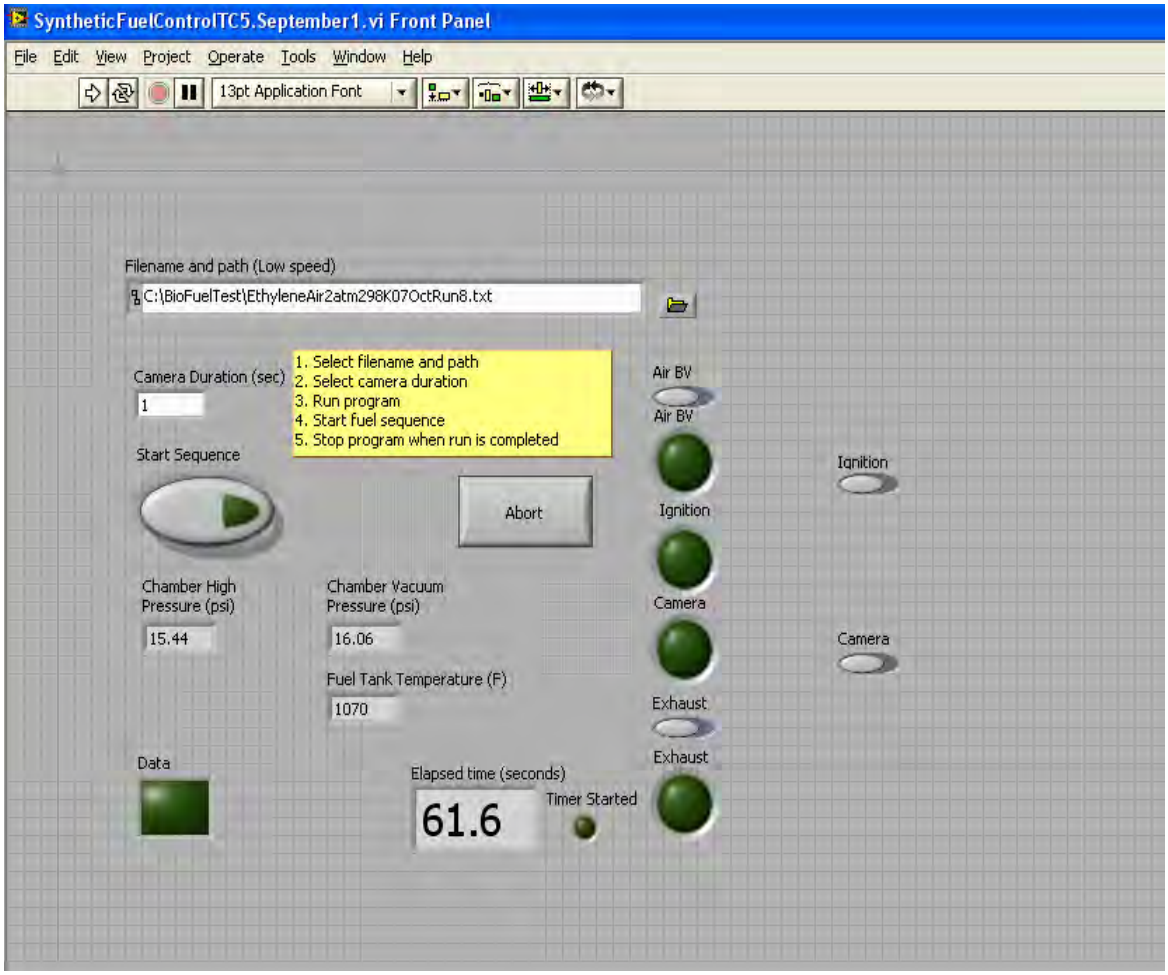

Figure 30. National Instruments LabView GUI

The GUI pictured in Figure 30 sets all the parameters for the camera trigger, ignition delay times and the chamber purge sequence. Once the desired fuel/air ratios were set manually, the camera and spark ignition is

triggered by depressing the “Start Sequence” button on the GUI. The program provides for a 10 second countdown prior to ignition to provide for a safe standoff. A standard operating procedure used to ensure proper startup, proper sequence for ignition, and to provide a safe condition directly after a runwas complete as well as for a complete shutdown of the chamber.

THIS PAGE INTENTIONALLY LEFT BLANK

III. EXPERIMENTAL METHOD AND DATA REDUCTION

A. SPHERICAL BOMB METHOD

This research uses the constant pressure spherical bomb method to determine the laminar flame speeds. The laminar flame speed is traditionally defined as the velocity that a planar flamefront travels relative to the unburned gas in a direction normal to the flame surface.

The constant pressure method uses a Schlieren system to view the flame front propagation history of an expanding spherical flame in a large confined chamber. This flame propagation is observed to identify any instability that may develop over the flame surface.

The effect of the flame stretch on the laminar flame speed and unstretched laminar flame speed are highly dependent on the unburned Markstein length. The stretched flame speed S_L with respect to the burned mixture is determined from the flame front history dr_f/dt using Equation (1).

$$S_L = \frac{dr_f}{dt}\left(\frac{\rho_b}{\rho_u}\right) \tag{1}$$

where ρ_b/ρ_u is the density ratio between the burned and unburned mixtures assumed to be in equilibrium and calculated using CEQUEL code.

The flame stretch rate K for the spherical flame due to the effects of curvature and flame motion is calculated using Equation (2).

$$K = (2/r_f)\, dr_f/dt \tag{2}$$

where r_f is instantaneous flame radius at time t.

The linear relationship between the stretch rate and the stretched burning laminar velocity was used to calculate the unstretched laminar burning velocity using Equation (3).

$$S_L = S_u - LK \tag{3}$$

where L is called the Markstein length corresponding to the sensitivity of S_u to the stretch rate. A linear extrapolation of S_L to zero stretch rate yields S_u values. The slope of the results yields the Markstein length. From the Markstein length the Markstein number Ma can be calculated from Equation (4).

$$Ma = L/\delta_D \tag{4}$$

where δ_D is the local characteristic flame thickness based on the stretched flame speed and the mass diffusivity D_u of the fuel in the unburned gas.

$$\delta_D = D_u/S_L \tag{5}$$

B. DATA REDUCTION

Through the optical window access of 152.4 mm a flame radius was measured from 16 to 61 mm. The pressure change inside the combustion chamber during the growth of the spherical flame from initiation until the flame reached the maximum viewing distance was observed to be constant. The

images were then processed using a MATLAB® code and angle measurement GUI (Figures 31 and 32). The corresponding flame radii were determined by measuring from the flame center perpendicular outward from the electrodes to the flame.

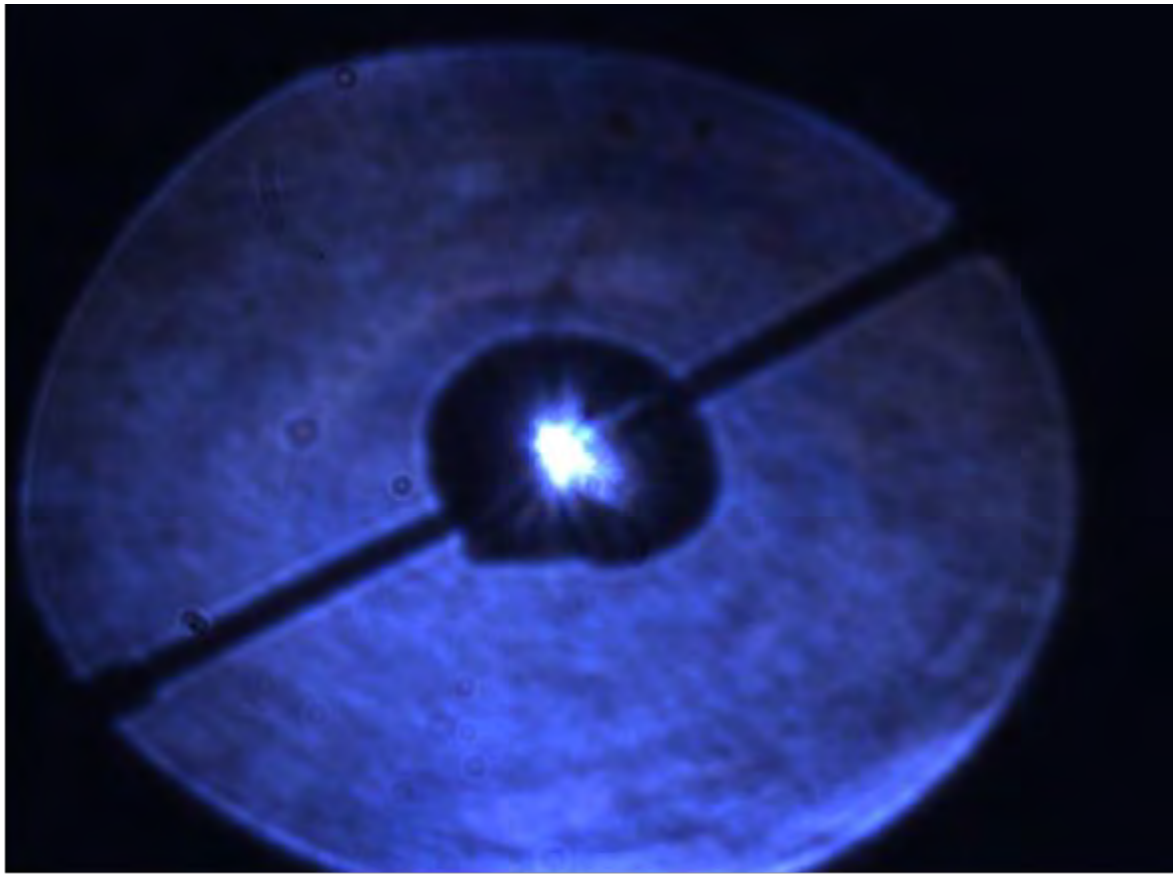

Figure 31. Original Image of Ethylene/Air mixture of Φ=1.

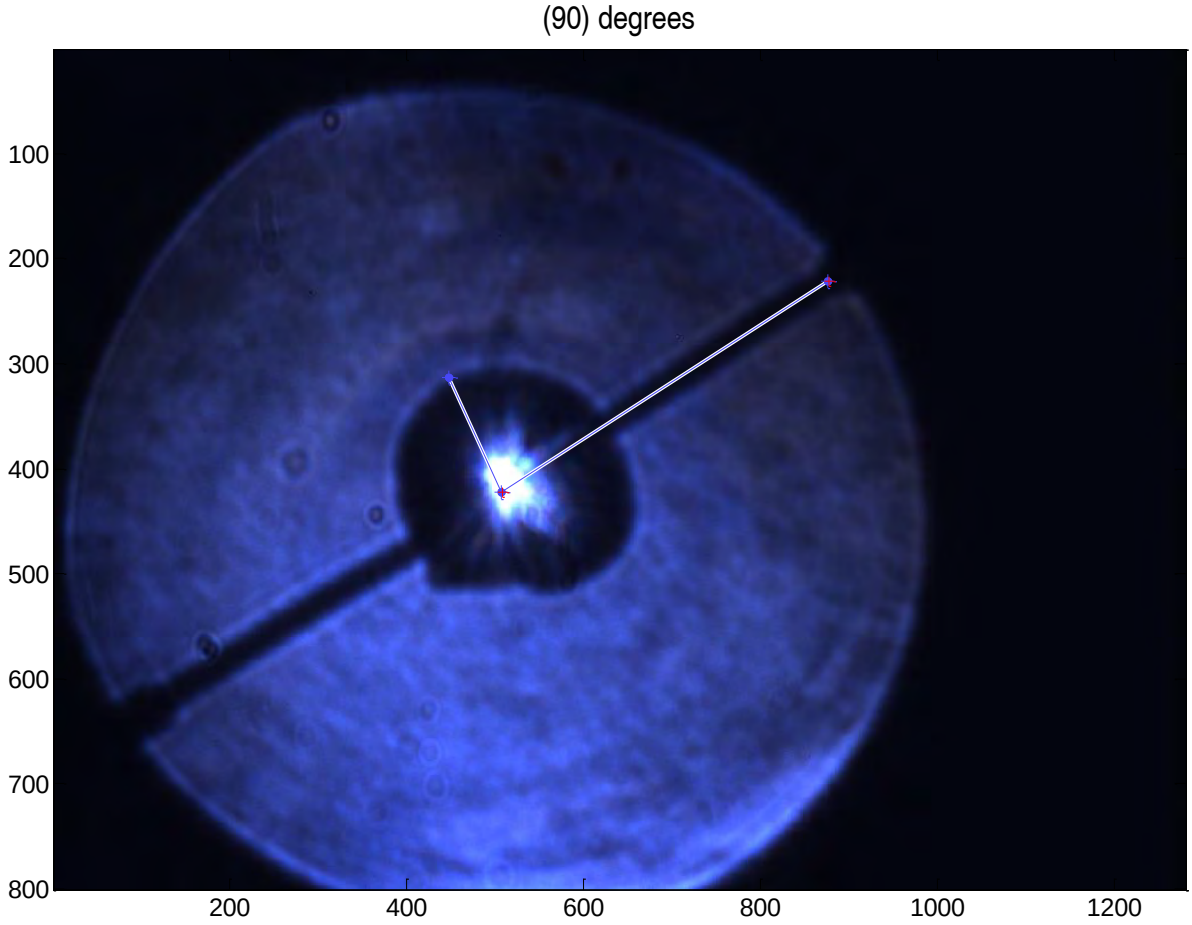

Figure 32. Image of Ethylene/Air Mixture of Φ=1, using Matlab Angle Measurement Tool.

The flame speeds were then calculated as the first order derivative of two consecutive flame radii with respect to time. The calculated flame speed using 2 points was slightly scattered and wavy in nature. As noted by Prathap et al. [11] to remove the local disturbances and waviness the time and flame speed data was processed using the MATLAB® curve fitting tool. A LOWESS (low weighted scatter plot smoothing) algorithm was then applied with a window size of 0.35.

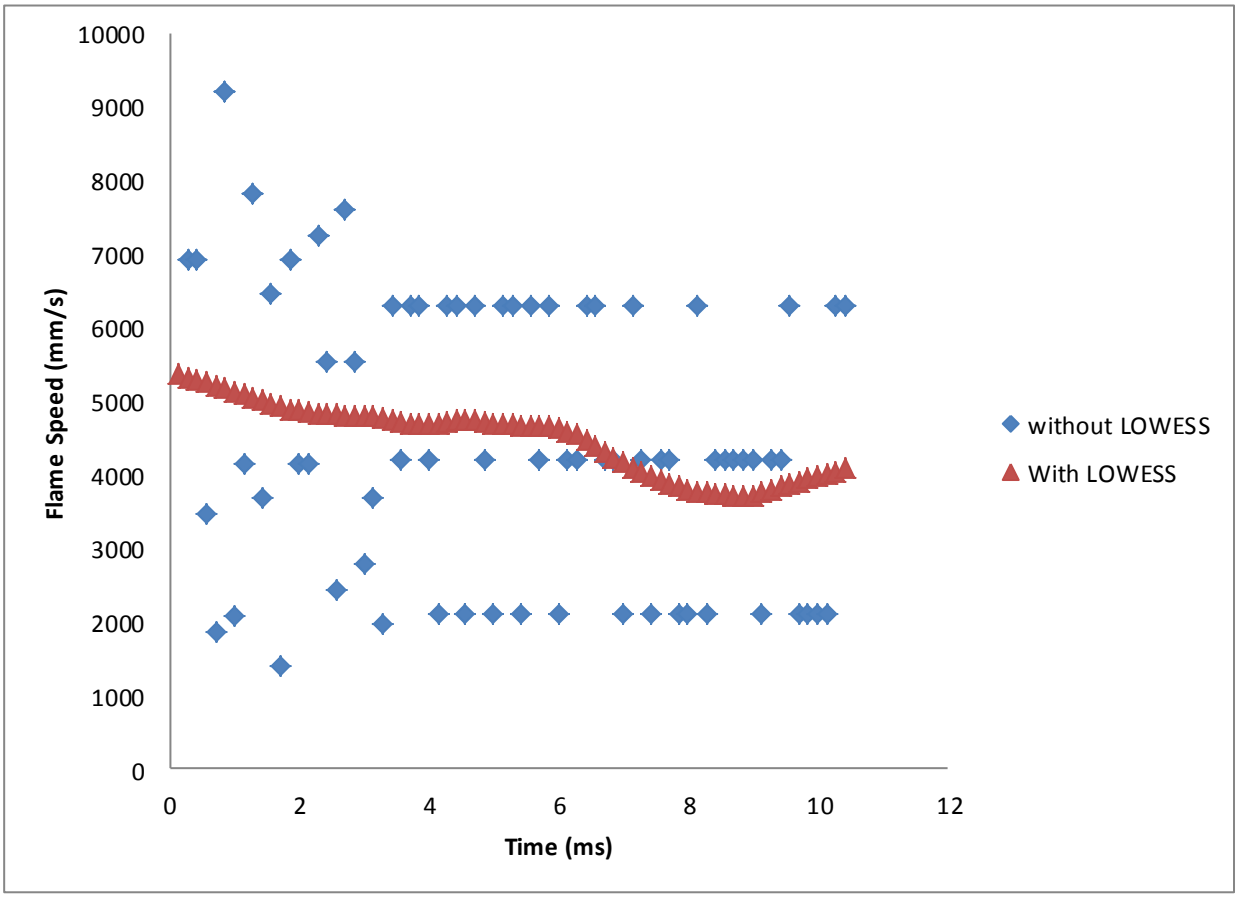

Figure 33. Flame speed as a Function of Time for Ethylene/Air mixture of Φ=1.1 Before and After Using LOWESS algorithm.

The density ratios of the burned gases were determined assuming the products to be in equilibrium, using CEQUEL. The smoothed flame speed and density ratio was then used to calculate the stretched burning velocity from Equation 1 and the flame stretch rate from Equation 2.

The stretched burning velocity was then plotted as a function of the stretch rate as shown in Figure 34. The data was again analyzed and potential ignition and wall disturbances were removed. The remaining data was then selected to obtain an R-squared value of 0.90 or greater.

As shown in Figure 35 the unstretched burning velocity was then obtained from the linear relationship of the stretched

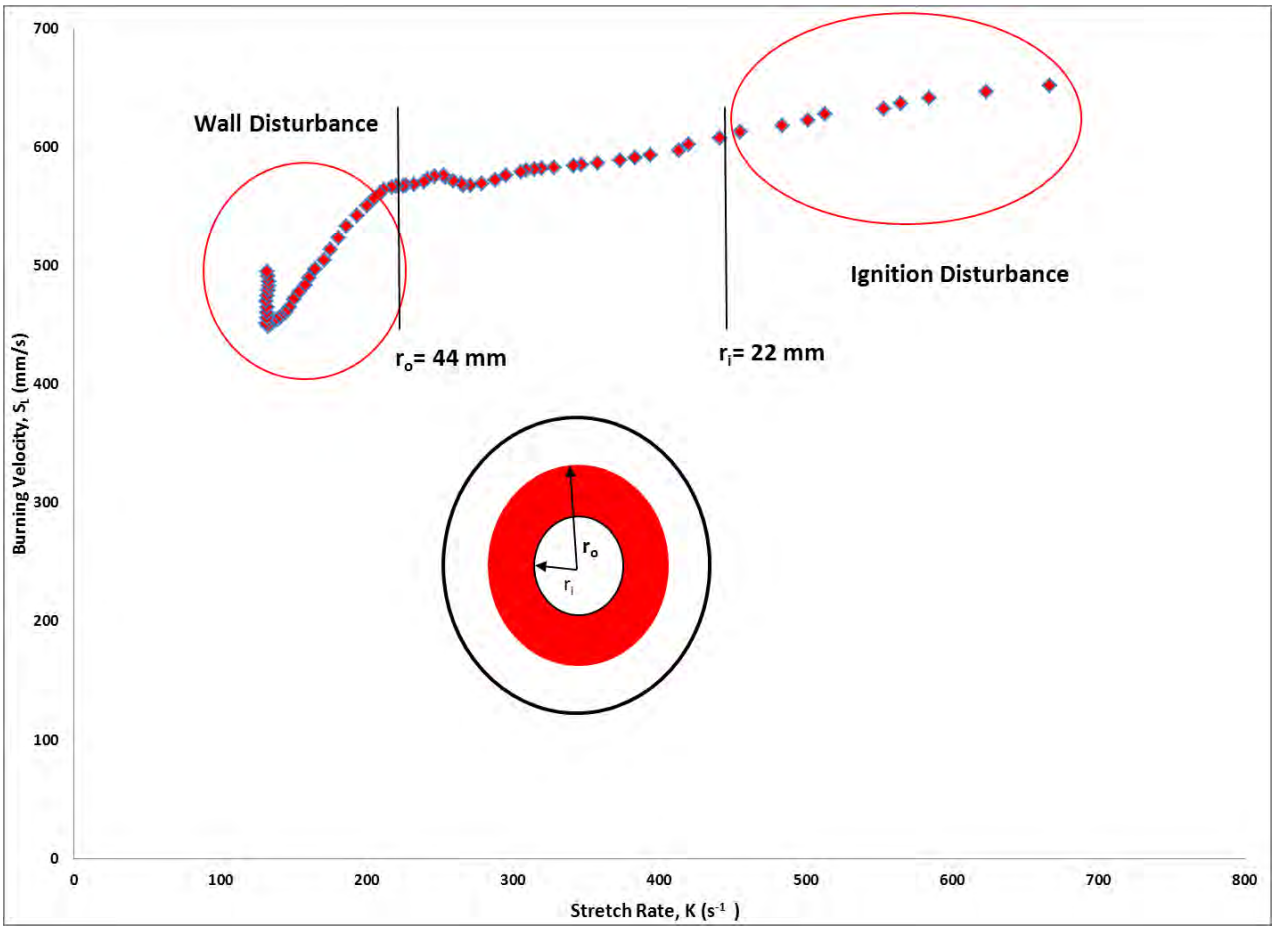

Figure 34. Stretched Burning Velocity as a Function of Stretch Rate for Ethylene/Air Mixture of Φ=1.1.

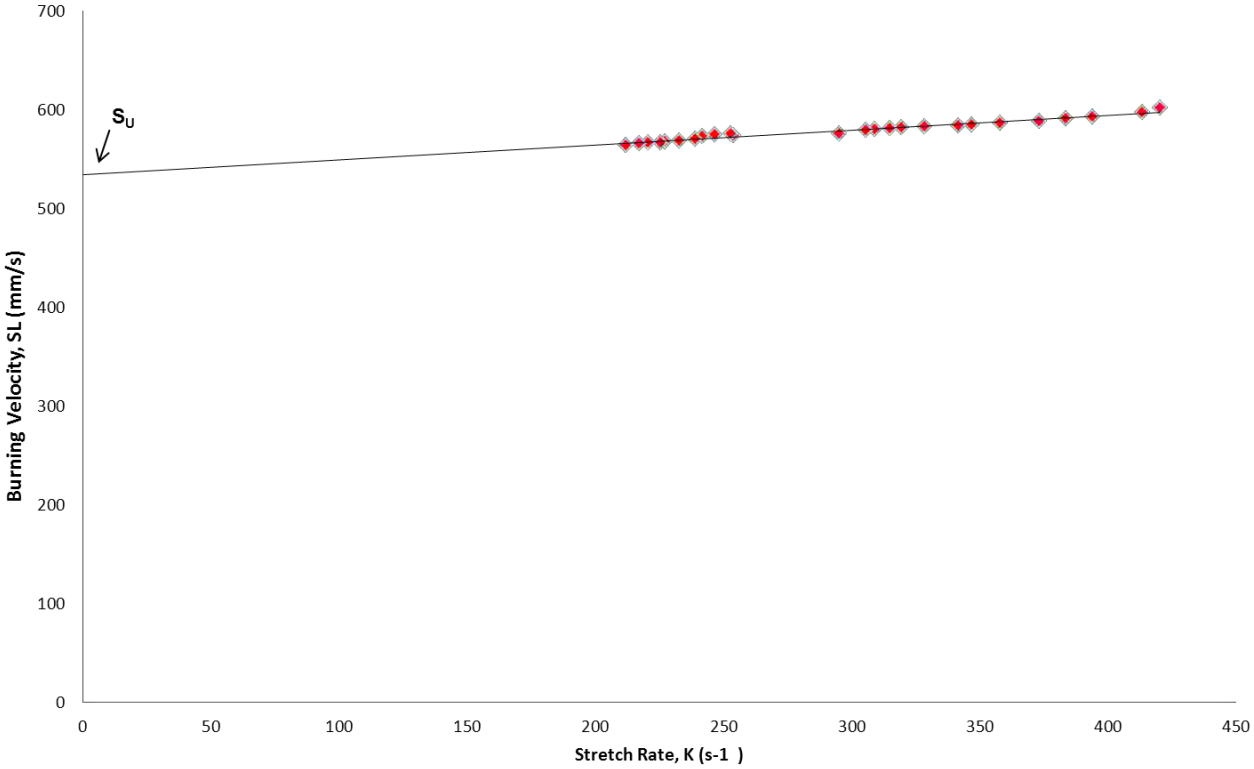

Figure 35. Extrapolated Stretched Burning Velocity as a Function of Stretch Rate for Ethylene/Air mixture of Φ=1.1 to yield Unstretched Burning Velocity.

This process was used for Ethylene/air mixtures at 2 atm with equivalence ratios ranging from 0.8 to 1.5, as tabulated in Table 1, to calibrate and verify proper post-processing procedure.

THIS PAGE INTENTIONALLY LEFT BLANK

IV. EXPERIMENTAL RESULTS AND DISCUSSION

The experimental conditions and results for ethylene/air mixture at an initial temperature of 298K, initial pressure of 2 atm and fuel equivalence ratio ranging from 0.8 to 1.5. Laminar burning velocities were measured as discussed earlier and compared with experimental results of Hassan et al. [6]. The comparison of present experimentation with those from literature will serve for validation. Table 1 shows the summary of test conditions such equivalence ratios with their associated unstretched laminar burning velocity, Markstein length and R-squared coefficient.

Table 1. Summary of Test Conditions

	Φ	ρ_b/ρ_u	D_u [mm^2/s]	S_u [mm/s]	L	R^2
C_2H_4/Air (T=298K)	0.8	0.1353	15.8	427	-0.938	0.94
	1	0.1190	15.8	530	-0.447	0.97
	1.1	0.1214	15.8	551	-0.236	0.975
	1.4	0.1209	15.8	464	-0.339	0.9
	1.5	0.1235	15.8	359	-0.49	0.965

A. UNSTRETCHED LAMINAR FLAME SPEED

As mentioned in the previous section the unstretched burning velocity is found by the linear extrapolation of the stretched burning velocity to a zero stretch rate. An example of this process was shown in Figure 35.

Figure 36 shows the present unstretched laminar burning velocities for ethylene/air mixtures as a function of fuel equivalence ratio at 2 atm. also shown are the experimentally determined burning velocities from Hassan et al. using the spherical bomb method.

The present data trend is in good agreement with the variation of the laminar flame speed with equivalence ratio for hydrocarbons. As Figure 36 shows the peak of the flame speed occurs at stoichiometric conditions or slightly fuel-rich mixture. Hassan et al. [6] has the peak flame speed occurring at the fuel-rich mixture of 1.2.

The comparison between measurements and those of Hassan et al. is seen to be in good agreement over the test range. The burning velocities are 3, 5.4 and 5% less for equivalence ratio of 0.8, 1 and 1.1, respectively. The burning velocity at equivalence ratio of 1.4 was found to be 3.1% higher than that of Hassan et al. [6]

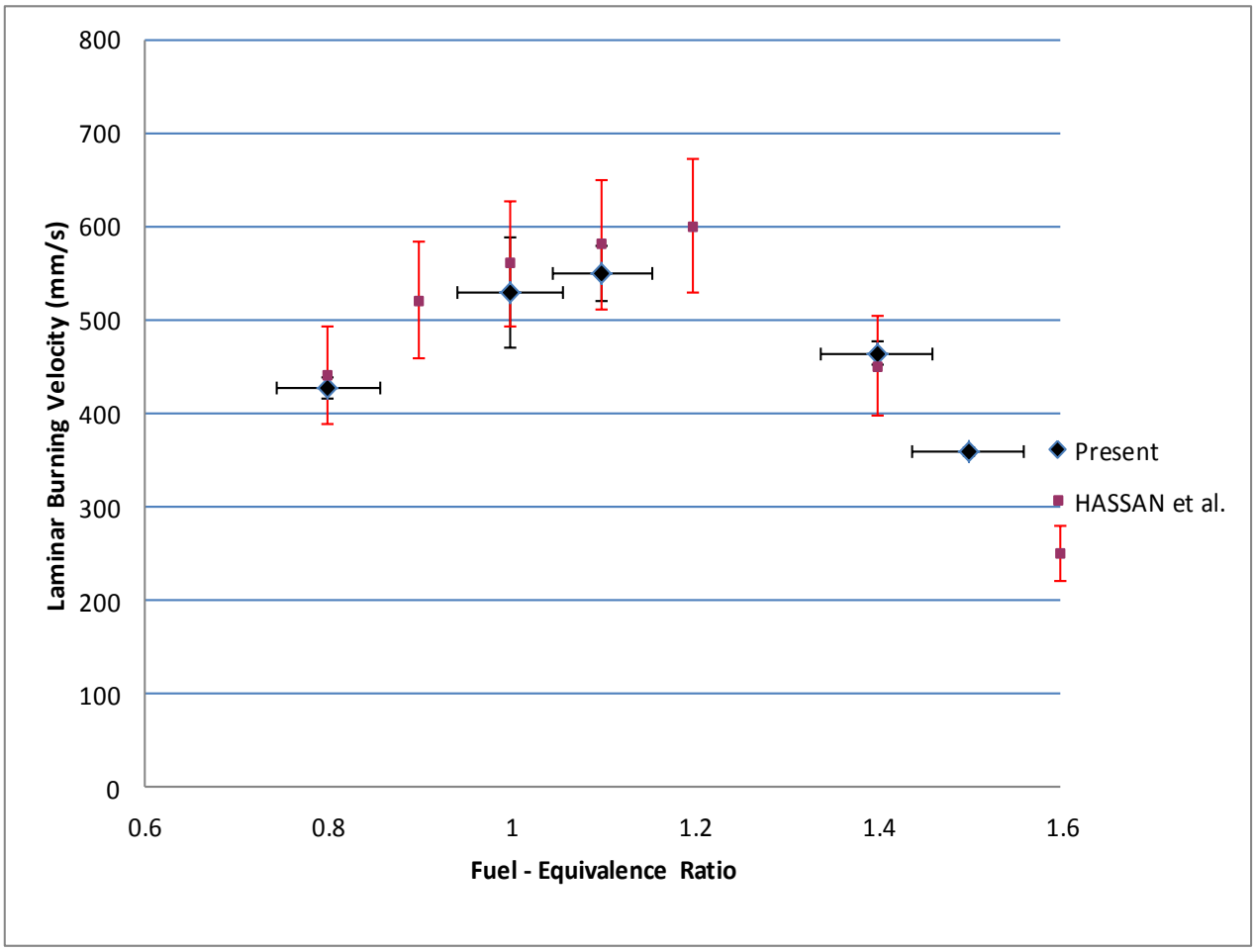

Figure 36. Measured Unstretched Burning Velocities as a Function of Equivalence Ratios. Measurements of Hassan et al [6] and Present Experiment.

B. MARKSTEIN NUMBER

The slope of this straight line fit of Equation 4 is defined as the Markstein length. The negatives value of the Markstein length indicates unstable flames and increased preferential diffusion instabilities. The Markstein number is calculated from the measure Markstein Length using Equation 4. Figure 37 shows the calculated Markstein number as a function of equivalence ratio at 2 atm and 298K. The data of Hassan et al are also plotted on the same figure. The mass diffusivity of ethylene reported by Hassan et al.

[5] was used for the calculations. The present Markstein number values are much lower than those reported by Hassan et al. [5] at all equivalence ratios. The present values as well as those reported by Hassan et al. [5] indicate negative Markstein length for all equivalence ratios. It is currently unsure why there is such a disparity in the Markstein Number values however, the present values could be quite sensitive to the flame radii considered to obtain the linear fit and associated R-squared. Hassan et al. [6] did not report this information.

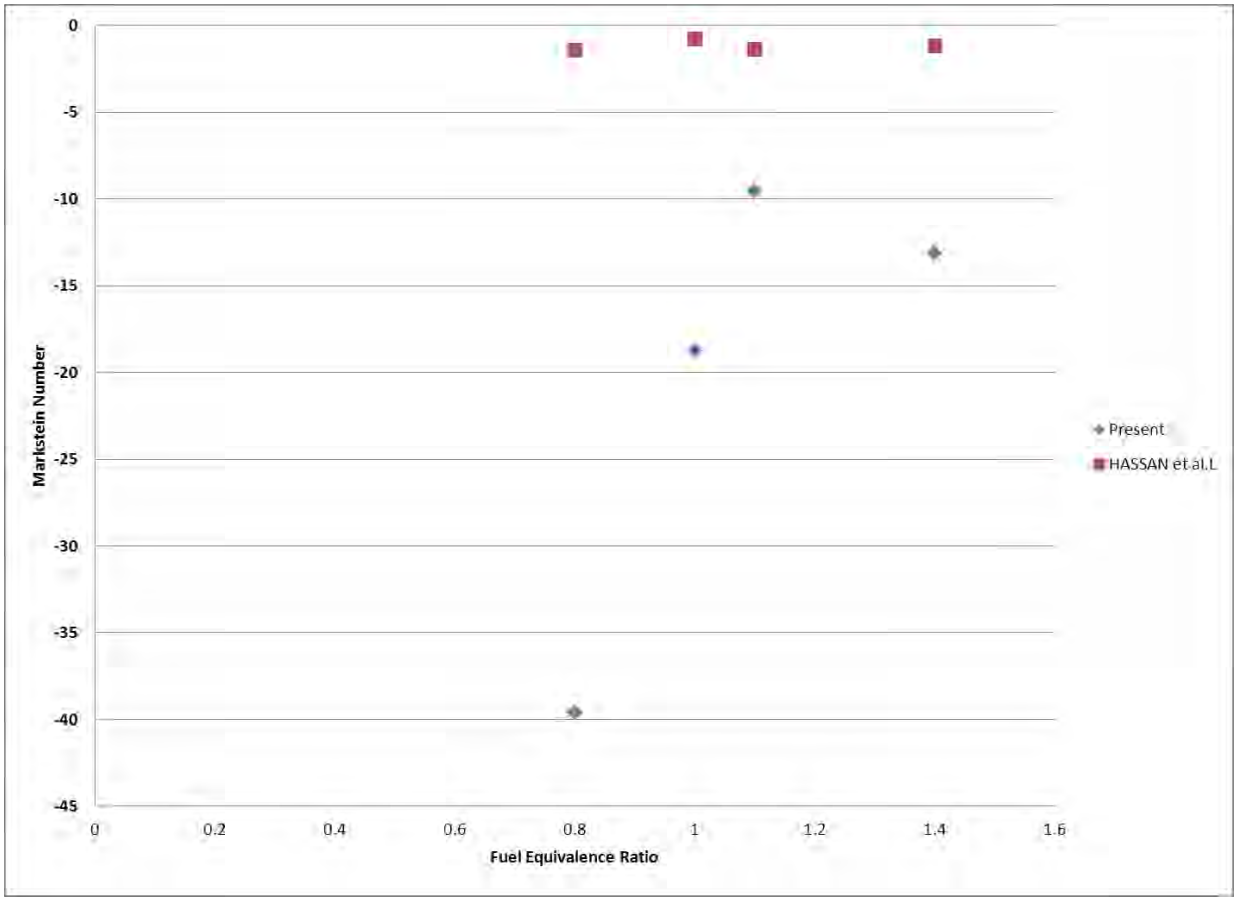

Figure 37. Measured Markstein Numbers as a Function of Equivalence ratio for Ethylene/Air. Measurements of Hassan et al. [6] and the Present experiment.

C. UNCERTAINITY ANALYSIS

An analysis was made to determine the total error associated with equipment accuracies and human error. The uncertainty of the flame radius is estimated to on the order of 1 pixel, which represents 0.22 mm. The uncertainty of the time used to calculate the flame speed is taken to be equal to the inverse of the frame rate, which is 0.31 ms. The error associated with the fuel equivalence ratio, as shown by the X error bars in Figure 34, is due to the Omega controllers used to monitor the partial pressure fill of the combustion chamber. The controllers have a display

precision that result in ± 0.1 Psia inaccuracy. The inaccuracy in controller precision lead to an uncertainty in equivalence ratios equal to; 0.8 ± 0.057, 1 ± 0.057, 1.1 ± 0.054, 1.4 ± 0.061 and 1.5 ± 0.061.

The unstretched laminar burning velocities were determined by taking the mean of 3 to 4 experimental runs. The Y error bars shown in Figure 34 shows the associated standard errors. The burning velocities had a standard error of 427 ± 11.1 mm/s, 530 ± 59.2 mm/s, 550 ± 29.5 mm/s, 464 ± 12.5 mm/s and 359 ± 4 mm/s.

V. CONCLUSION AND FUTURE WORK

A. CONCLUSION

1. A laboratory-based high pressure combustion chamber was designed and fabricated with the intention of measuring laminar flame speeds of F-76, JP-5, HRJ and HRD in support of the US Navy's alternative fuels test program. To validate the combustion chamber design, instrumentation, and post processing procedure the laminar burning velocities of ethylene/air mixtures at a pressure of 2 atm, temperature of 298K and fuel equivalence ratios ranging from 0.8 to 1.5 were measured and compared to published data.

2. The results from experimental tests revealed that the present data trend is in good agreement with the variation of the laminar flame speed with equivalence ratio for hydrocarbons. The comparison between present experimental results and those of Hassan et al. was found to be in good agreement over the range of conditions evaluated. The burning velocities were 3, 5.4 and 5% less for equivalence ratio of 0.8, 1 and 1.1, respectively. The burning velocity at equivalence ratio of 1.4 was found to be 3.1% higher than that of Hassan et al

3. An attempt was made to measure the laminar flame speed for F-76 at a pressure of 5 atm and temperature of 500K. It was discovered that due to the vapor characteristics of F-76 auto ignition conditions were met prior to premix conditions.

B. FUTURE WORK

1. Dynamic Injection

Auto ignition of the fuel could possibly be eliminated by redesigning the high pressure combustor chamber to include four high pressure diesel injectors. This will allow the fuel to be dynamically injected into the preheated chamber, just below ignition temperature, and ignited with the preexisting electrodes.

To verify the chemical composition and physical properties of the liquid fuels throughout the experiment spectroscopy instrumentation should be included in the redesign. The current optical window access already provides the means to accomplish these measurements.

2. Phase Doppler Particle Analyzer

A second viable option to measuring the laminar burning velocity would be utilize a Phase Doppler Particle Analyzer (PDPA). Standard Navy fuels and their potential replacements are relatively dense and to achieve near engine conditions they must be heated and pressurized to fairly high pressures. A PDPA could be flexible enough to handle these requirements.

APPENDIX A: STANDARD OPERATING PROCEDURES

Standard Operating Procedures
Test Cell #5

RUN Setup Procedures

1) On TC#5 desktop Computer (next to control panel)
   a) "National Instruments Lab View" – OPEN
   b) "SyntheticControlTC5.September1.vi" – OPEN
      1. Change data file name as needed, right click data file, select "Data Operations", select "Make Current File Default", File – SAVE
2) Verify power to the 120 V auxiliary and fuel tank heating system-plugged in (outlet 1)
3) Verify power to the 240 VAC heating system- knife edge in up position
4) Turn on power to control panel-(switch AC 1)
5) Turn on power to air/exhaust actuators-(Switch AC 2)
6) Verify power to 1600W light source-knife edge in up position-(Switch 2)
7) Restore power to high speed Camera
8) On TC#5 Schlieren System laptop
   a) Open camera software
   b) verify frame rate per second and shutter rate for test
9) Turn on Arc lamp power supply (Oriel
10) Verify service needle valve for 0-50 psia transducer (Kulite XTEL-190-15A) is in the open position.
11) Verify oil pressure in vacuum pump

Run Profile

1) Verify set points on heat tape controllers- 500°F
2) Heat chamber (for liquid fuels) and lines for approximately 1 hour or until temperature reach 500°F. (may need to recycle system after 15 minutes)
3) Place the chamber under vacuum:
   a. Ensure vacuum needle valve is in the closed position.
   b. Restore power to the vacuum pump-plugged in
   c. Check for adequate vacuum pressure via mechanical gage.
   d. Open needle valve to begin evacuating the chamber
   e. Once under vacuum secure needle valve.

f. Secure Vacuum-unplug

4) Manually open the fuel fill severe service needle valve, slowly, until predetermined partial pressure is met and then secure valve.
5) Isolate 0-50 psia pressure transducer
6) Actuate air solenoid valve and fill until testing pressure and equivalence ration is met.
7) for Lab Personnel – NOTIFY OF IMPENDING TEST
8) LabView Program –RUN
9) Exit test cell
10) Countdown (Beginning with 10 second count from after the start sequence is initiated)
11) High Speed Data Recording – START
12) Spark ignition (for approximately 100ms)
13) High Speed Data Recording – STOPS
14) Air purge valve- OPEN
15) Exhaust valve- OPEN
16) Air/Exhaust valves-CLOSED
17) Sequence complete.

Run Shutdown Procedure

1) LabView Program –STOP
2) If securing for the day secure power to heating system and allow chamber to cool.
3) Secure light source (never secure via main power button)
    a. Turn lamp off via lamp off button and allow lamp to cool
    b. Once lamp has cooled secure power source via main switch on control panel.
    c. secure power to the light source via knife edge switch on breaker
4) Secure power to the 120 V auxiliary and fuel tank heating system.
5) Secure power to spark ignition system.
6) Secure power to the 240 V heating systems -.
7) Close the testing program and power down the Lab View® computer.
8) Power down the laptop for image capturing.
9) Power down high speed camera

APPENDIX B: COMBUSTION CHAMBER ASSEMBLY DRWAINGS

Figure 38. Combustion Chamber Overview

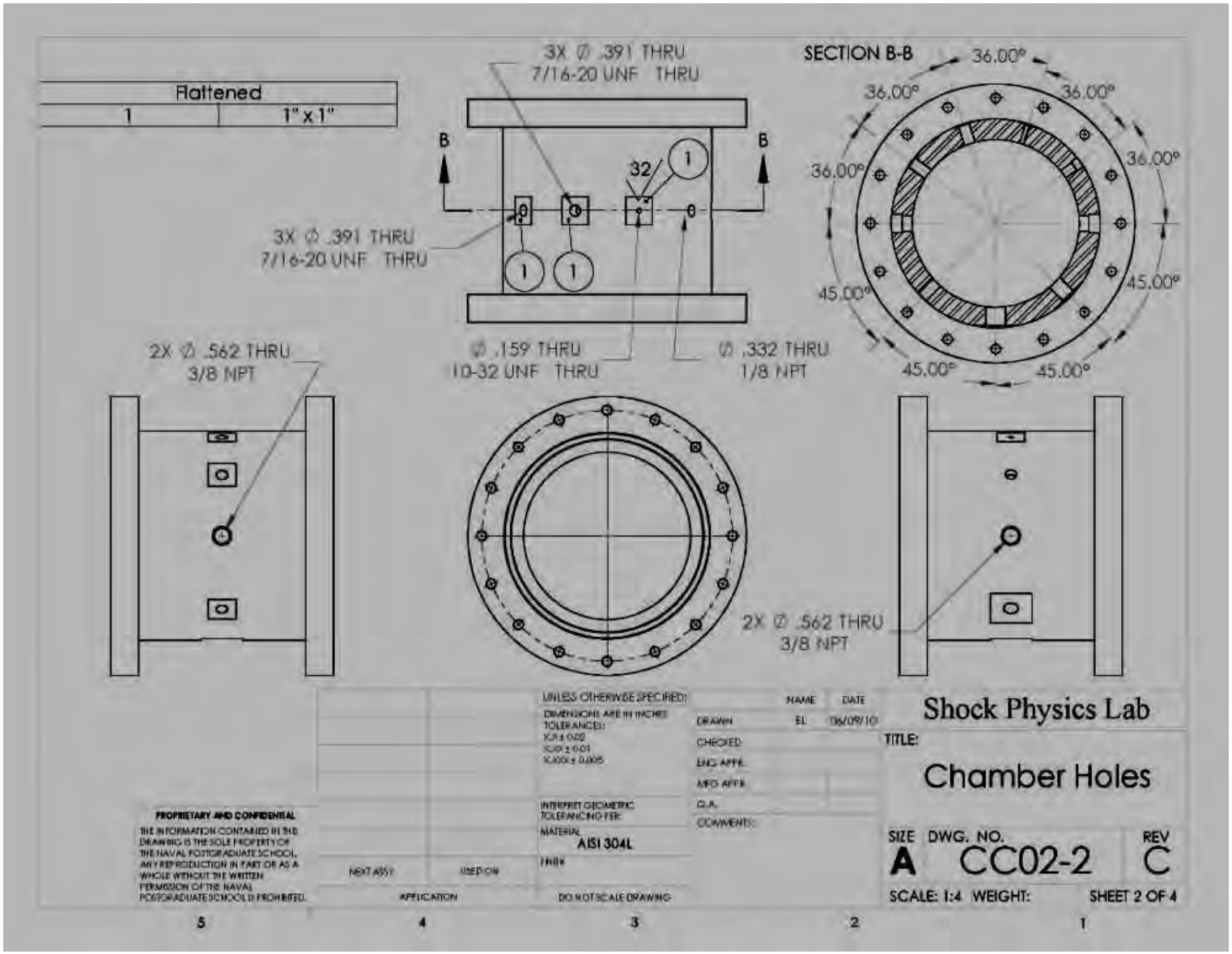

Combustion Chamber-Holes (1 of 2)

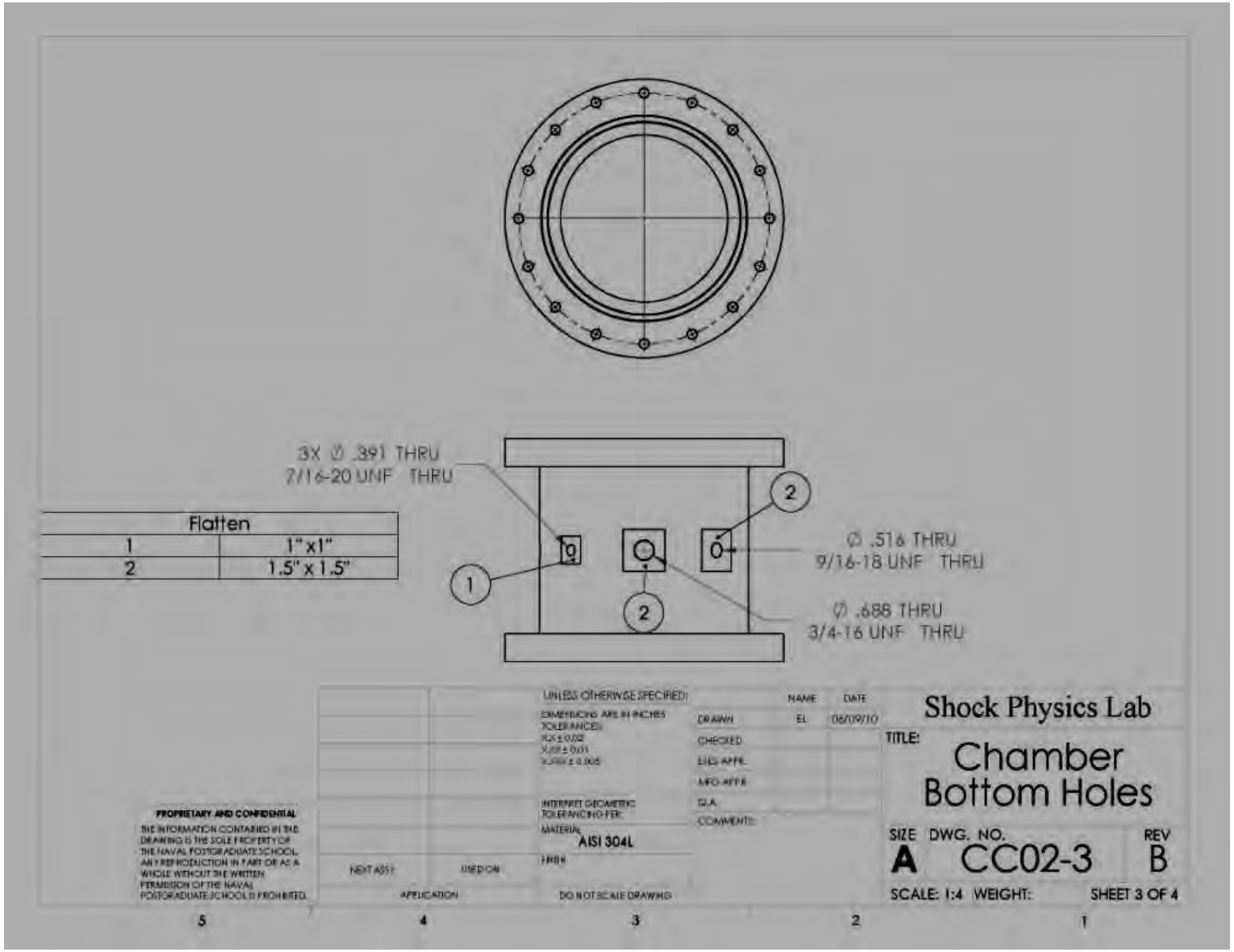

Figure 39. Combustion Chamber-Holes(2 of 2)

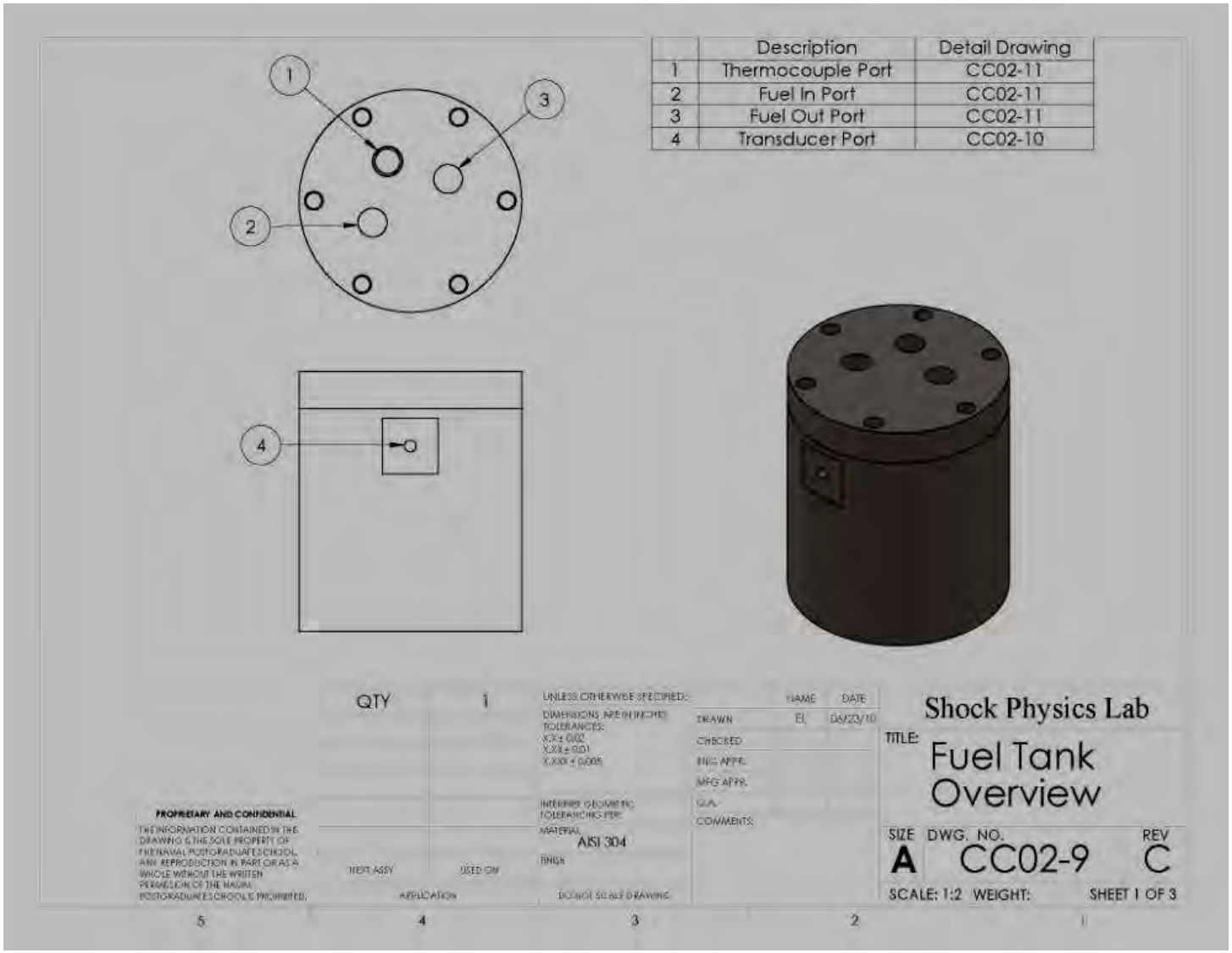

Figure 40. Fuel Tank Overview (1 of 2)

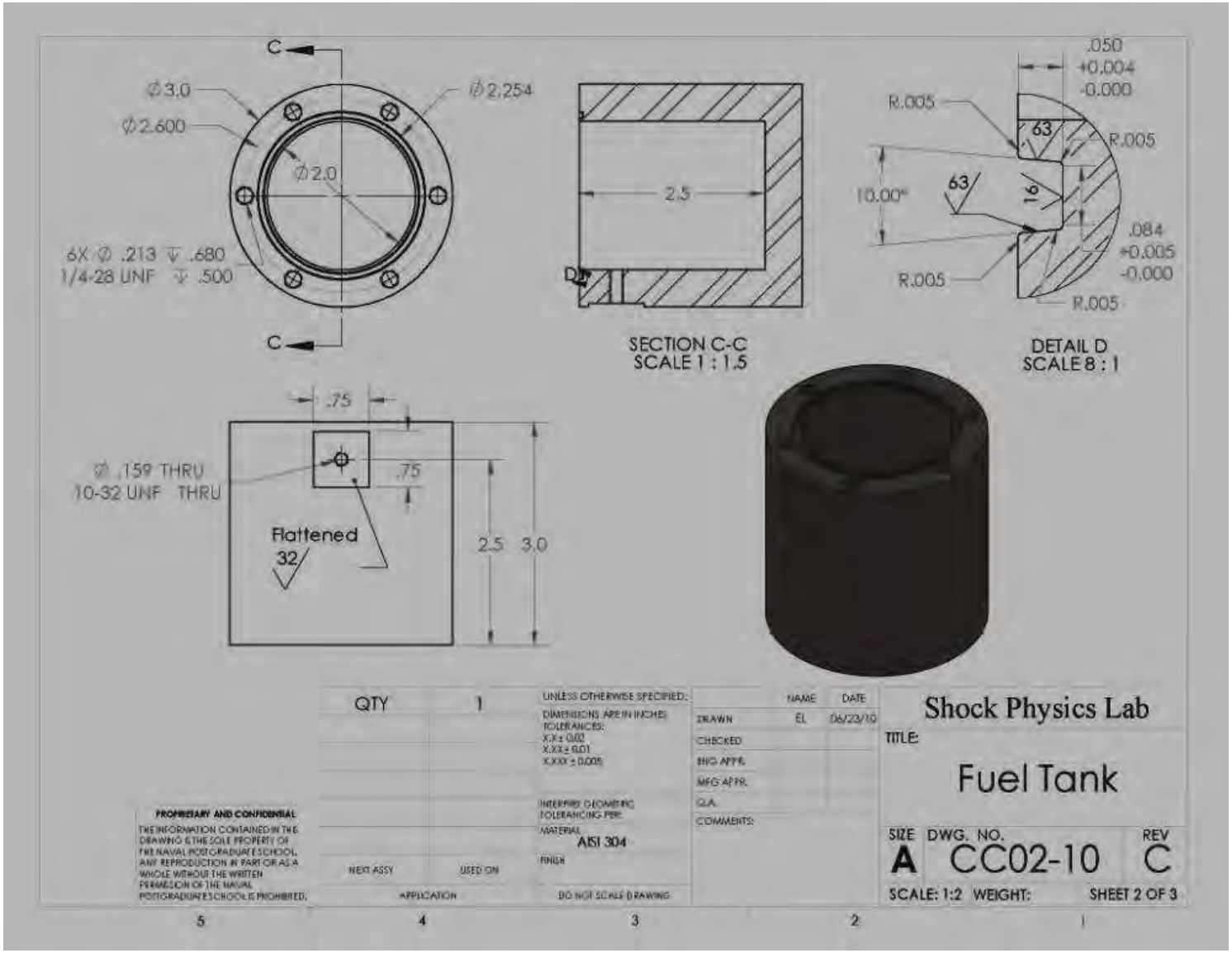

Figure 41. Fuel Tank (2 of 2)

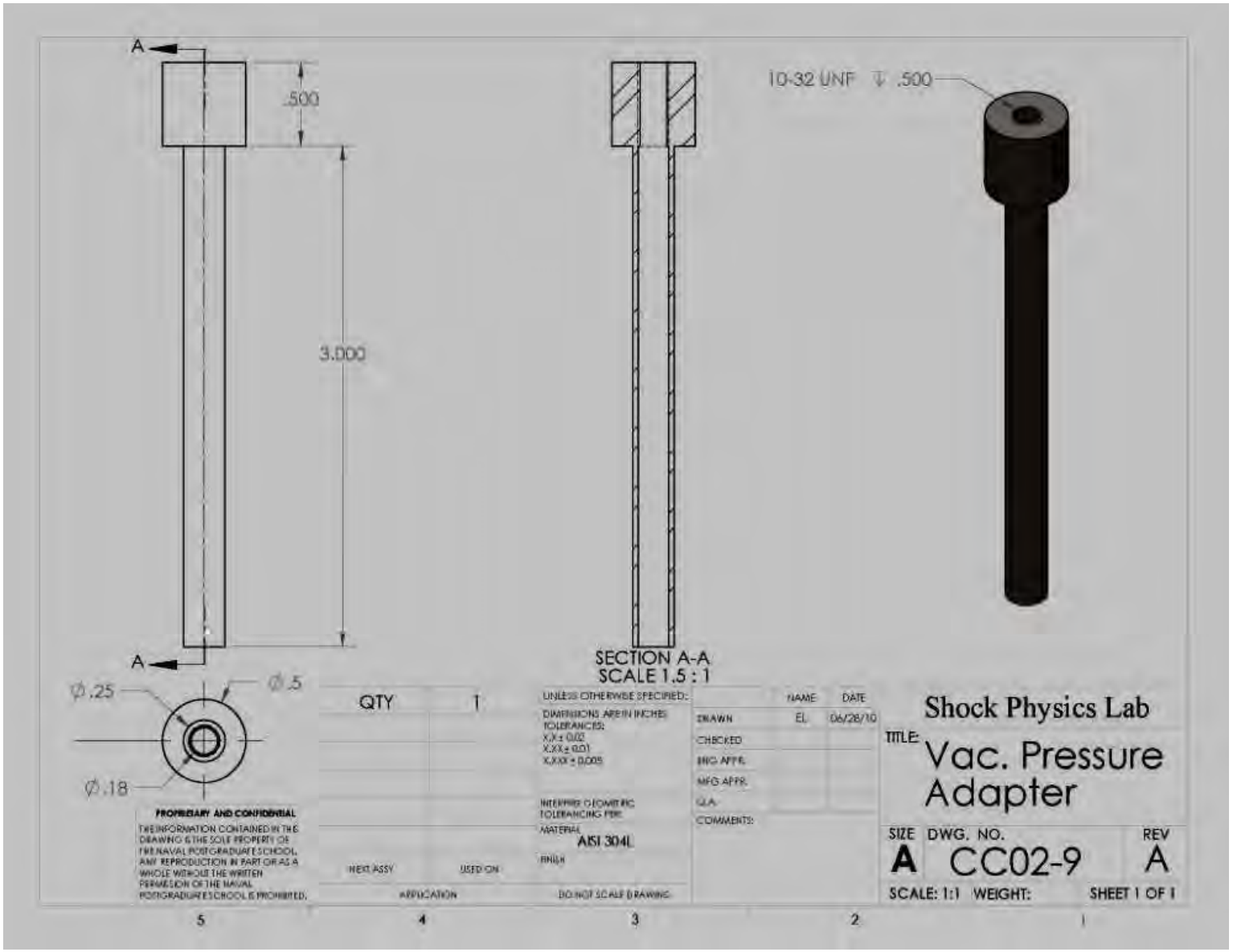

Figure 42. Vacuum Pressure Adapter

LIST OF REFERENCES

[1] J. T. Bartis, and L. V. Bibber, "Alternative Fuels for Military Applications," Internet: www.**rand**.org/content/dam/**rand**/pubs/monographs/.../**RAND** May 13, 2011.

[2] Office of Naval Research Public Affairs, "Navy Secretary Announces Ambitious Energy Goals," Oct. 16, 2009.

[3] T. Edwards, C. Moses, and F. Dryer, "Evaluation of Combustion Performance of Alternative Aviation Fuels," 46th AIAA/ASME/SAE/ASEE Joint Propulsion Conference and Exhibit, Nashville, TN, July 2010.

[4] T. M. Vu, "Using Expanding Spherical Flames Method To Measure The Unstretched Laminar Burning Velocities Of LPG-Air Mixtures," *Science and Technology Development*, Vol 12, No. 08, 2009.

[5] K. K. Kuo, "Premixed Laminar Flames" in *Principles of Combustion*, New York: John Wiley and Son, 1976, pp.309-322.

[6] M. I. Hassan, K. T. Aung, O. C. Kwon, and G. M. Faeth, "Properties of Laminar Premixed Hydrocarbon/Air Flames at Various Pressures," *Journal of Propulsion and Power*, Vol.14, No. 4, August 1998.

[7] K. T. Aung, M.I. Hassan, and G. M. Faeth, ''Flame/Stretch Interactions of Laminar Premixed Hydrogen/Air Flames at Normal Temperature and Pressure,'' *Combustion and Flame*, Vol. 109, No. 1, 1997, pp. 1–24.

[8] S. C. Taylor, ''Burning Velocity and Influence of Flame Stretch,'' Ph.D. Dissertation, University of Leeds, England, UK, 1991.

[9] F. N. Egolfopoulos, D. L. Zhu, and C. K. Law, ''Experimental and Numerical Determination of Flame Speeds: Mixture of C2-Hydrocarbons with Oxygen and Nitrogen,'' *23rd Symposium (International)on Combustion*, The Combustion Inst., Pittsburgh, PA, 1990, pp. 471–478.

[10] F. N. Egolfopoulos, C. Jig, and Y. L. Wang, "Flame Studies of Conventional and Alternative Jet Fuels," *Journal of Propulsion and Power*, Vol.27, No. 4, Aug. 2011.

[10] C. Prathap, A. Ray, and M. R. Ravi, "Investigation of Nitrogen Dilution Effects on the Laminar Burning Velocity and Flame Stability of Dry Syngas Fuel at Atmospheric Condition, "*Combustion and Flame*, Vol. 155, Issue 1-2, October 2008, pp. 145-160.

INITIAL DISTRIBUTION LIST

1. DefenseTechnicalInformationCenter
   Ft. Belvoir, Virginia

2. Dudley Knox Library
   Naval PostgraduateSchool
   Monterey, California

3. Knox Millsaps
   Chairman, Mechanical and Aerospace Engineering
   Naval Postgraduate School
   Monterey, California

4. Christopher Brophy
   Department of Mechanical and Aerospace Engineering
   Naval Postgraduate School
   Monterey, California

5. Martin Quinones
   Naval Surface Warfare Center, Carderock Division
   Philadelphia, Pennsylvania

6. Andrea Vigliotti
   Naval Surface Warfare Center, Carderock Division
   Philadelphia, Pennsylvania

7. Sharron Beerman
   Office of Naval Research
   Arlington, Virginia